JOURNAL OF GEOPHYSICAL RESEARCH, VOL. 114, D14204, doi:10.1029/2008JD011128, 2009

Evaluation of tropical and extratropical Southern Hemisphere African aerosol properties simulated by a climate model

Brian I. Magi,[1,2] Paul Ginoux,[2] Yi Ming,[2] and V. Ramaswamy[2]

Received 8 September 2008; revised 7 May 2009; accepted 15 May 2009; published 23 July 2009.

[1] We compare aerosol optical depth (AOD) and single scattering albedo (SSA) simulated by updated configurations of a version of the atmospheric model (AM2) component of the NOAA Geophysical Fluid Dynamics Laboratory general circulation model over Southern Hemisphere Africa with AOD and SSA derived from research aircraft measurements and NASA Aerosol Robotic Network (AERONET) stations and with regional AOD from the NASA Moderate Resolution Imaging Spectroradiometer satellite. The results of the comparisons suggest that AM2 AOD is biased low by 30–40% in the tropics and 0–20% in the extratropics, while AM2 SSA is biased high by 4–8%. The AM2 SSA bias is higher during the biomass burning season, and the monthly variations in AM2 SSA are poorly correlated with AERONET. On the basis of a comparison of aerosol mass in the models with measurements from southern Africa, and a detailed analysis of aerosol treatment in AM2, we suggest that the low bias in AOD and high bias in SSA are related to an underestimate of carbonaceous aerosol emissions in the biomass burning inventories used by AM2. Increases in organic matter and black carbon emissions by factors of 1.6 and 3.8 over southern Africa improve the biases in AOD and especially SSA. We estimate that the AM2 biases in AOD and SSA imply that the magnitude of annual top of the atmosphere radiative forcing in clear-sky conditions over southern Africa is overestimated (too negative) by ~8% while surface radiative forcing is underestimated (not negative enough) by ~20%.

Citation: Magi, B. I., P. Ginoux, Y. Ming, and V. Ramaswamy (2009), Evaluation of tropical and extratropical Southern Hemisphere African aerosol properties simulated by a climate model, *J. Geophys. Res.*, *114*, D14204, doi:10.1029/2008JD011128.

1. Introduction

[2] Biomass burning is a major source of particulate matter in the atmosphere and influences global aerosol optical depth (AOD) and single scattering albedo (SSA). Burning processes release a significant number of particles that absorb incoming sunlight [e.g., *Reid et al.*, 2005b], which warms the polluted layer of the atmosphere, and scatter sunlight back into space, which acts to cool the surface [e.g., *Magi et al.*, 2008]. The cooling and warming together may affect local, regional, and even global atmospheric dynamics, but in order to determine the impact of the aerosol on dynamics, it is important to evaluate the simulation of aerosol properties in biomass burning regions in global-scale general circulation models (GCMs). In the larger sense, evaluations of aerosol radiative effects are also important because GCMs are used to simulate past, present, and future climates [*Intergovernmental Panel on Climate Change*, 2007]. Uncertainties in the estimates of climate sensitivity are strongly related to the continuing difficulties in measuring and modeling aerosol physical and chemical properties [*Schwartz*, 2004; *Andreae et al.*, 2005].

[3] The Southern Hemisphere African aerosol loading is strongly affected by seasonal biomass burning [e.g., *Eck et al.*, 2003; *Swap et al.*, 2003; *Ito et al.*, 2007]. In terms of the contribution to global fire occurrence, analysis from the NASA Moderate Resolution Imaging Spectroradiometer (MODIS) satellite collection 4 fire product [*Giglio et al.*, 2003, 2006] suggest that Africa alone accounts for about 44% of the millions of fires that occur every year on the entire planet (Figure 1). The satellite observations of fire occurrence are confined to the most recent decade or so, while in situ data focusing on biomass burning emissions have been collected in Africa during field campaigns like SAFARI-92 [*Scholes et al.*, 1996], EXPRESSO [*Ruellan et al.*, 1999], SAFARI-2000 [*Haywood et al.*, 2003a, 2003b; *Hobbs et al.*, 2003; *Schmid et al.*, 2003], and most recently during DABEX in the western Sahel [*Johnson et al.*, 2008]. Southern and northern hemisphere Africa account for similar proportions of the annual fires in Africa, and nearly all those fires occur in the tropics. Although fire emissions are directly linked with fire occurrence, emissions are also dependent on a range of parameters such as vegetation density, type, and moisture content, and thus are not uniquely related to fire occurrence [*van der Werf et al.*, 2006].

[4] The majority of the aerosol mass emitted from biomass burning is carbonaceous in nature [*Eatough et al.*, 2003;

[1] Atmospheric and Oceanic Sciences Program, Princeton University, Princeton, New Jersey, USA.
[2] Geophysical Fluid Dynamics Laboratory, NOAA, Princeton, New Jersey, USA.

0148-0227/09/2008JD011128$09.00

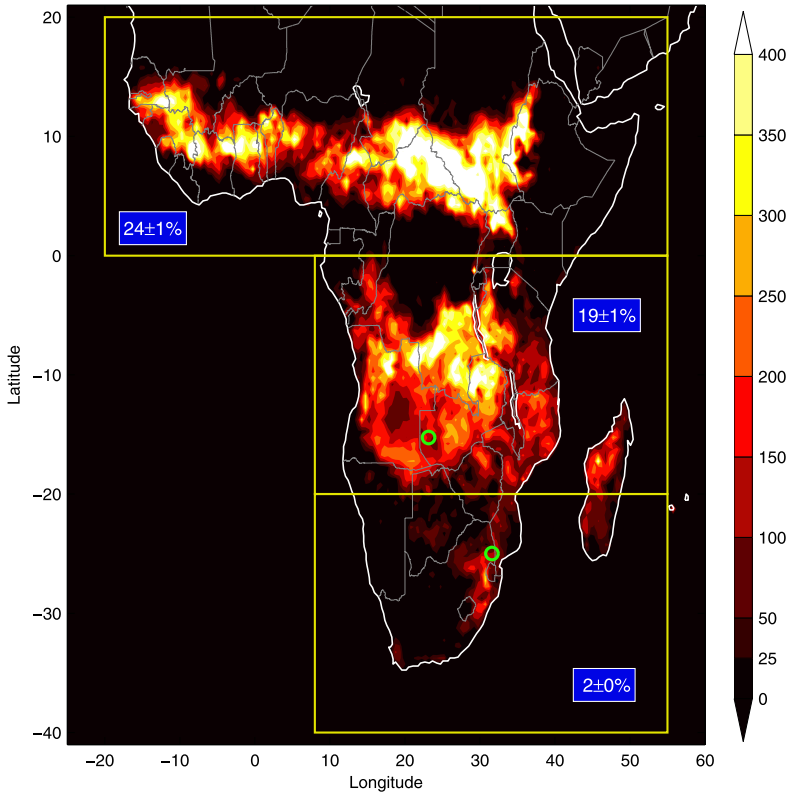

Figure 1. Annual fire counts in Africa averaged from 2001 to 2006 using measurements from the NASA MODIS satellite (collection 4). The numbers in the blue boxes are the mean (±standard deviation of the 6 year mean) contribution of the particular yellow-boxed regions to global annual fire counts. The green circles are the two AERONET sites referred to in this study (Mongu, Zambia at 15.25°S, 23.15°E; Skukuza, South Africa at 24.99°S, 31.59°E). The color bar units are number of fires per year in a 0.5° latitude by 0.5° longitude grid box.

Formenti et al., 2003; *Gao et al.*, 2003; *Kirchstetter et al.*, 2003; *Reid et al.*, 2005a], and carbonaceous particles are known to both strongly scatter and absorb solar radiation [*Bond and Bergstrom*, 2006]. Estimates by *Bond et al.* [2004] suggest that, on average, 86% of the carbonaceous aerosol emissions in Africa are from biomass burning, whereas only 59% of carbonaceous aerosol emissions in the rest of the world are from biomass burning (noting that this number is only 46% if we exclude South America). Thus, carbonaceous aerosol emissions from most regions of the world are due to processes other than biomass burning. Estimates by *Bond et al.* [2004] also suggest that biomass burning from Africa alone contributes to nearly 30% of the total global carbonaceous aerosol emissions every year, which includes emissions from fossil fuel, biofuel, and biomass burning.

[5] The burning in Africa occurs consistently every year. The relative contribution of Southern Hemisphere tropical Africa fire counts to total global fire counts derived from MODIS measurements [*Giglio et al.*, 2003, 2006] ranges from 17 to 21%, with actual fires detected ranging from 271,000 to 309,000 per year (Figure 1). Monthly fire counts from MODIS show that burning begins in the tropics in May, peaking in intensity from July to September. MODIS fire counts in extratropical southern Africa peak in August and September and range from 20,000 to 42,000 per year, which is about half the fire counts reported for the United States and Canada. The factor of 2 fluctuation in the extratropical fire counts is partly due to variations in rainfall which directly controls the amount of vegetation available to burn [*Anyamba et al.*, 2003; *van der Werf et al.*, 2004]. The fires that occur every year in southern Africa may have regional impacts on cloud properties and atmospheric circulation, so it is important that simulations of the aerosol in that region are closely evaluated against available measurements.

[6] In this study, we evaluate AOD and SSA over southern Africa simulated by the second version of the Atmospheric Model (AM2) component of the NOAA Geophysical Fluid Dynamics Laboratory (GFDL) GCM [*GFDL Global Atmospheric Model Development Team*, 2004; *Delworth et al.*, 2006]. We will discuss output from two versions of AM2, which we call AM2e and AM2i, where the "e" and "i" refer to an externally mixed and internally mixed aerosol, respectively. We describe this and other major features in section 2, and also highlight some of the many changes between the version of AM2 used here and the version described by *Ginoux et al.* [2006] in a previous evaluation of simulated aerosol properties. To evaluate the output from AM2, we use independently derived data sets collected from the University of Washington research aircraft [*Hobbs et al.*, 2003] during the SAFARI-2000 field campaign [*Magi et al.*, 2003; *Schmid et al.*, 2003], retrieved using the ground-based NASA Aerosol Robotic Network or AERONET [*Holben et al.*, 2001; *Dubovik et al.*, 2002], and retrieved using radiance measurements from the NASA MODIS satellite

[*Remer et al.*, 2005; *Levy et al.*, 2007]. The comparisons are thus on multiple temporal and spatial scales to gauge whether comparisons are consistent. We present the comparisons in section 3, where we focus some of the comparisons (AERONET and MODIS in sections 3.2–3.3) on the months with peak fire activity from about July to September as discussed above. The readers should note that we found that peak aerosol loading in the region occurs one to two months after peak fire activity, so this limitation should be considered with respect to our results. We analyze the results in section 4 and our conclusions are in section 5.

2. Model Description

[7] In this study, we analyze output from the second version of the Atmospheric Model (AM2) of the GFDL GCM [*GFDL Global Atmospheric Model Development Team*, 2004]. AM2 has a resolution of 2° latitude by 2.5° longitude with 24 vertical levels and are driven by monthly mean observed sea surface temperature fields. The model results are saved every 24 h from January 2000 to December 2006, except in the comparison with aircraft data (section 3.1) where the model output is saved every 3 h from August to September 2000. The last month of a separate 20-year simulation (1980–2000) is used as the initial condition for GCM experiments described in this study.

[8] Since the evaluation of simulated global aerosol properties by *Ginoux et al.* [2006], AM2 has significantly changed. Below we describe many new features included in the version of AM2 used in this study without directly comparing them with the version of AM2 in the study by *Ginoux et al.* [2006]. We discuss similarities and differences between results in this study and those by *Ginoux et al.* [2006] in section 4.5. Some of the major changes are the method of nudging to meteorology, online aerosol fields that interact directly with other physical components of the model, and aerosol optical properties. We describe these changes and other aspects of the updated version of AM2 below.

[9] The dynamical fields of AM2 are "nudged" toward the reanalysis fields from NCEP (National Center for Environmental Prediction) using a relaxation method with a 6 h relaxation time scale [*Moorthi and Suarez*, 1992]. This procedure ensures that the meteorology in the model mimics as best as possible the present-day known patterns. The main impact of this in southern Africa is to significantly improve correlation between aerosol properties from AM2 output and observations, with a secondary impact being to decrease root-mean-squared differences (usually by ~10%).

[10] AM2 contains the following modules for aerosol simulation: emission, which includes sulfate, dust, organic carbon, black carbon, and sea salt emissions (see section 2.1); chemistry, which currently uses a prognostic equation for H_2O_2 with prescribed OH, HO_2, O_3, and NO_3 fields simulated with MOZART-2 [*Horowitz et al.*, 2003] for gaseous sulfur oxidations; advection, which is computed by a finite volume dynamical core [*Lin*, 2004]; boundary layer turbulent mixing, which uses a second-order closure scheme [*GFDL Global Atmospheric Model Development Team*, 2004]; moist convection [*Arakawa and Schubert*, 1974]; dry deposition, which includes gravitational settling as a function of aerosol particle size, hygroscopicity and air viscosity [*Chin et al.*, 2002] and surface deposition as a function of surface type and meteorological conditions [*Wesely*, 1989]; and wet deposition, which accounts for the scavenging of soluble species in convective updrafts and rainout/washout in large-scale precipitation [*Giorgi and Chameides*, 1986; *Balkanski et al.*, 1993].

2.1. Aerosol Sources

[11] AM2 simulates major tropospheric aerosol types [e.g., *Kinne et al.*, 2006], including sulfate, dust, organic carbon (OC) as organic matter (OM), black carbon (BC), and sea salt. Sulfate is mostly formed by oxidation of sulfur dioxide (SO_2) emitted from fossil fuel and biomass burning combustion. SO_2 fossil fuel emissions are based on energy statistics for the year 2000 as described by *Dentener et al.* [2006]. We use monthly fire emissions of SO_2 based on Version 2 of the Global Fire Emission Database (GFED) [*van der Werf et al.*, 2006]. In addition to direct emission, SO_2 is produced from the oxidation of dimethylsulfide (DMS) released from the ocean. DMS emission is based on the parameterization proposed by *Chin et al.* [2002].

[12] The carbonaceous aerosol emissions (OM and BC) from biomass burning are based on GFED monthly data, while annual emissions from biofuel and fossil fuel burning are based on the inventory for the year 2000 developed by *Dentener et al.* [2006]. OM is calculated as 1.4 × OC for biomass burning, as recommended by *Dentener et al.* [2006]. Secondary organic aerosol (SOA) formed by oxidation of volatile organic compounds are also simulated and are assumed to result from the oxidation of α-pinene ($C_{10}H_{16}$) and n-butane (C_4H_6), on the basis of *Guenther et al.* [1991]. We use the same reaction rates as the ones proposed by *Tie et al.* [2005]. The aging of carbonaceous aerosols are treated as in the work by *Reddy and Boucher* [2004] with an exponential lifetime of 1.63 days.

[13] Dust emission follows the parameterization by *Ginoux et al.* [2001], and is based on the preferential location of sources in topographic depression. *Li et al.* [2008] described the dust component and examined the impact of simulated dust transport on Antarctica. In southern Africa, the major source is the Kalahari desert with maximum activity in summer [*Prospero et al.*, 2002]. Sea salt particles are emitted from the ocean according to *Monahan et al.* [1986], but the aerosol in the region described in this study is not strongly affected by sea salt.

2.2. Aerosol Properties

[14] We analyze output from AM2 with two configurations: "AM2e" aerosol optics are based on an externally mixed aerosol, while "AM2i" internally mixes all sulfate and BC using volume-weighted refractive indices [e.g., *Chylek et al.*, 1988]. In this study, if we refer to AM2 without an "e" or "i," we intend the discussion in that case to apply to both configurations of AM2. If discussions are specific to AM2e or AM2i, we use the "e" or "i" designation.

[15] Aerosol extinction and absorption are a function of aerosol size distribution, extinction efficiency, and single scattering albedo (SSA) and are determined from offline Mie theory [*Bohren and Huffman*, 1983] calculations. The size distributions of sulfate and carbonaceous aerosols are simulated as lognormal, while dust and sea salt mass distributions are constant within five bins ranging from

Table 1. Assumed Aerosol Properties in AM2e[a]

Species	D_g (μm)	σ_g	Density (g/cm^3)	MEC (m^2/g)[b]	SSA[b]
Sulfate	0.100	2.00	1.77	5.60	1.000
OC	0.170	1.49	1.80	3.22	0.965
BC	0.0236	2.00	1.00	9.27	0.209

[a]D_g, geometric mean diameter; σ_g, geometric standard deviation; MEC, mass extinction cross section; and SSA, single scattering albedo.
[b]At 550 nm, 50% RH.

0.02 to 20 μm diameter. Aerosol properties for sulfate, OM, and BC as simulated by AM2 are listed in Table 1. AM2 dust and sea salt properties are discussed by *Li et al.* [2008] and *Ginoux et al.* [2006], respectively.

[16] BC from both fossil fuel and biomass burning is assumed to be 80% hydrophobic and 20% hydrophilic, whereas OM is 50% hydrophobic and hydrophilic, per *Ming and Russell* [2004]. Refractive indices for OM are based on *Hess et al.* [1998], and optical properties of BC are from *Haywood and Ramaswamy* [1998]. Sulfate is considered to be entirely neutralized by ammonium and the dependency of the refractive index on wavelength and relative humidity is based on *Tang and Munkelwitz* [1994]. Sea salt refractive indices and hygroscopic growth factors are both based on *Tang et al.* [1997]. Dust is simulated as hydrophobic and the optical properties are from *Balkanski et al.* [2007].

3. Comparisons

[17] In this section, we compare AM2 output to independently derived data sets from aircraft, AERONET, and MODIS. Two data sets (aircraft and AERONET) offer comparisons with both AOD and SSA, while the MODIS data set is limited to AOD. All comparisons of AOD and SSA are at a wavelength of 550 nm unless otherwise stated. We interpolated AERONET data to 550 nm from the reported wavelengths using the Angstrom exponent from the AERONET retrievals. Column-averaged SSA from the aircraft and from AM2 are weighted by aerosol extinction, providing values that are representative of the polluted lower layer of the atmosphere and that are comparable with AERONET SSA.

[18] Intercomparisons between the data sets used to evaluate AM2 are important to consider in the discussion that follows in sections 3.1–3.3. *Magi et al.* [2008] showed that the aircraft-derived AOD and SSA usually agreed to within uncertainty with AERONET AOD and SSA, but noted that a dedicated validation of AERONET SSA products has yet to be completed. MODIS AOD and aircraft-derived AOD agree to within uncertainties about 50% of the time for cases over southern Africa [*Magi et al.*, 2008]. Comparing the current version (collection 5) MODIS AOD products with AERONET AOD at various sites around the world, *Levy et al.* [2007] showed that median AOD from MODIS and AERONET agreed to within ~25%, with MODIS biased slightly high. However, for sites in southern Africa, MODIS AOD was biased low by about 30% (R. Levy, personal communication, 2008) showing that agreement depends on the details of the MODIS aerosol retrieval at a particular location (e.g., prescribed aerosol choices and/or assumed surface albedo). We show in Figure 2 that AERONET sites discussed in this study (Skukuza, South Africa, and Mongu, Zambia; see section 3.2) and MODIS regionally averaged AOD agree to within uncertainties and are significantly correlated, implying that even with spatial and temporal differences in sampling, the instruments see a similar seasonal cycle. AERONET and MODIS match more closely in the tropics than the extratropics because the burning is more uniform across the tropical region, whereas the MODIS extratropical regional average includes a significant area of Africa that does not burn (see Figure 1). Thus, the Skukuza AERONET AOD does not seem as representative of the extratropical region than the Mongu AERONET AOD does of the tropical region. In general, the confidence in AOD products (especially the direct sun data products) is higher than the confidence in SSA products, but both are widely referenced.

3.1. Aircraft

[19] We compare the total column AOD and column-averaged SSA simulated by AM2 (referred to as AM2e AOD and AM2e SSA, or AM2i AOD and AM2i SSA) in a $2^\circ \times 2.5^\circ$ grid cell with AOD and SSA derived from the University of Washington (UW) research aircraft vertical profiles (henceforth, UW AOD and UW SSA) in August and September 2000 [*Magi et al.*, 2003; *Schmid et al.*, 2003]. UW AOD and SSA are based on in situ measurements by combining nephelometry, absorption photometry, and sun photometry with data processing algorithms described by *Magi et al.* [2007, 2008].

[20] The UW vertical profiles were in an atmosphere impacted to varying degrees by smoke from local and regional biomass burning and, as a result, UW AOD ranged from 0.16 to 1.13 (median of 0.34) and UW SSA ranged from 0.81 to 0.93 (median of 0.87) over 20 separate cases [*Magi et al.*, 2008]. Thus, the comparison offers a sense of the ability of AM2 to simulate significant fluctuations in AOD and SSA, as well as an understanding of how representative UW vertical profiles (spatial scale of ~10 km) are of an entire AM2 grid cell (spatial scale of ~100 km). We construct this comparison by using the AM2 grid cell that encompasses the UW vertical profile and use 3-hourly AM2 output to find the best temporal match to the time of the UW vertical profile. We also discuss the spatial variability of AM2 output by analyzing the eight AM2 grid cells surrounding the central grid cell: we call this the neighboring grid cell variability.

[21] We show the correlation between AM2e AOD and UW AOD in Figure 3. The root-mean-squared (RMS) difference is 0.41 with a correlation coefficient (r^2) of 0.65 ($p < 0.05$, where p is defined as the probability that a random distribution would be better correlated with the data, and we assume that $p < 0.05$ is a significant correlation). In the overall sense, the correlation (r^2) of 0.65 implies that increases and decreases in measured AOD were fairly well simulated, but the RMS difference of 0.41 is greater than the median UW AOD of 0.34. The bias suggests that AM2e AOD is less than UW AOD by about 0.30. However, we have to examine this comparison on many levels since the spatial scales of the UW measurements are so much different than that of AM2e.

[22] Neighboring grid cell variability of AM2e AOD (shown as vertical error bars in Figure 3) does not explain

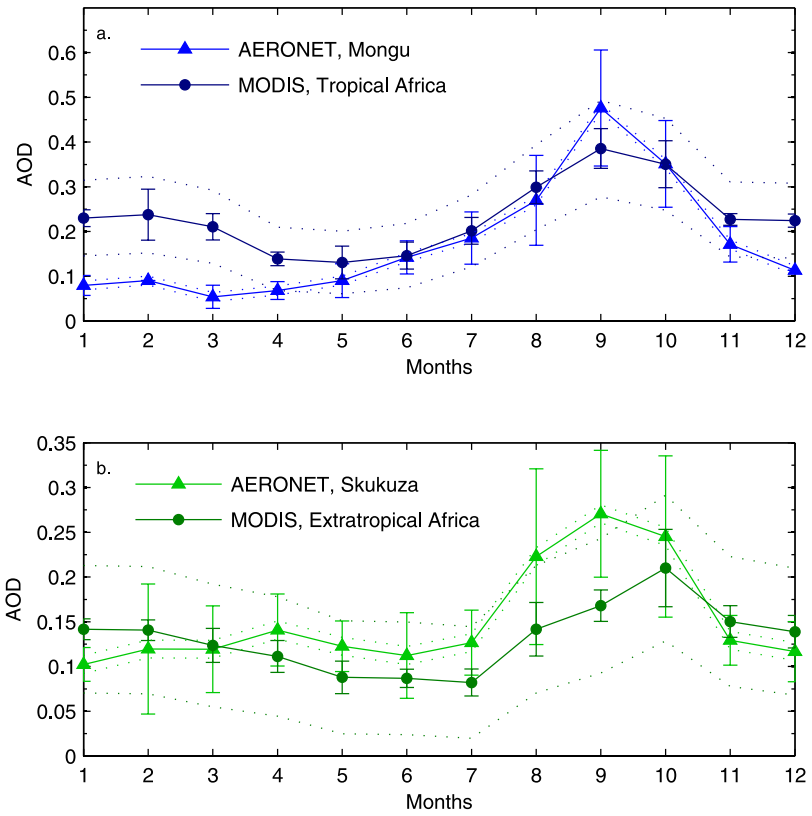

Figure 2. Comparison of monthly averaged aerosol optical depth (AOD) at a wavelength of 550 nm derived from AERONET and MODIS. We compare (a) Mongu, Zambia (latitude 15.25°S, longitude 23.15°E, elevation 1107 m) AOD (blue with triangles) with the average MODIS AOD (dark blue with circles) over the tropical region of southern Africa (0–20°S) and (b) Skukuza, South Africa (latitude 24.99°S, longitude 31.59°E, elevation 150 m) AOD (green with triangles) with the average MODIS AOD (dark green with circles) over the extratropical region (20–40°S). MODIS AOD is based only on land retrievals. Dotted lines are AERONET and MODIS retrieval product uncertainties (±0.01, ±0.05 ± 0.15 × AOD, respectively). Error bars are the standard deviation of the monthly mean (i.e., variability from 2000 to 2006 for a particular month). Correlation coefficients are $r^2 = 0.73$ and $r^2 = 0.44$, which are both significant at the 95% confidence level.

the discrepancy for high AOD (UW AOD > 0.4), but could be part of the reason for the differences at low AOD. Measurement and retrieval uncertainty in the UW AOD, shown as horizontal error bars in Figure 3 and discussed by *Magi et al.* [2008], is too small to explain the discrepancy. The RMS difference of 0.52 at tropical latitudes accounts for most of the total RMS difference of 0.41 mentioned above, where the mean AM2e AOD is 0.25 compared to the mean UW AOD of 0.67. MODIS fire counts (Figure 1) show that the tropical latitudes (0° to 22.5°S) of southern Africa are where the largest numbers of fires occur in any given year, and although large-scale climate variability like the phase of the El Nino–Southern Oscillation (ENSO) does have some impact on seasonal emissions [*Anyamba et al.*, 2003; *van der Werf et al.*, 2004], we would expect that the AOD over tropical southern Africa is correspondingly high every year during the biomass burning season. AM2e AOD is significantly correlated with UW AOD at tropical latitudes ($r^2 = 0.59$, $p < 0.05$) indicating that variability in biomass burning emissions may be captured by AM2e, but the large RMS difference suggests that either the burning emissions are too low, the optical properties of the AM2e aerosol (i.e., the properties used to translate aerosol mass concentrations to AOD) are incorrect, the aerosol sink is too strong, or the advective transport is too strong. We explore these mechanisms below.

[23] At extratropical latitudes (22.5°S to 40°S), the correlation between AM2e AOD and UW AOD is not significant ($r^2 = 0.11$, $p = 0.43$), and the RMS difference is 0.13, which is about 50% of the mean AOD for the eight data points. The lower aerosol loadings in the extratropics are mainly a result of fewer fires occurring in the region, although emissions from grassland burning are also lower owing to higher combustion efficiency [*van der Werf et al.*, 2006]. The extratropics can be more adversely affected by tropical burning emissions when a synoptic-scale event (like a strong frontal passage) [see *Garstang et al.*, 1996] transports smoke from the tropics over the extratropics. The simulation of AOD in the extratropics probably gives insight into the skill of AM2e simulation of aged or background aerosols. Most of the extratropics does not have enough vegetation (i.e., due to the Kalahari expanse and Namib desert) to make a strong contribution to overall biomass burning emissions, regardless of variations in the vegetation density due to factors like ENSO [*Anyamba et al.*, 2003; *van der Werf et al.*, 2004].

[24] In Figure 4, we show the comparison of AM2e SSA with UW SSA for both the tropics and the extratropics. Of the 20 comparisons, there are five when AM2e SSA is less than UW SSA, suggesting a fairly strong positive bias. The basic conclusion from this is that the aerosol simulated by AM2e is not absorbing enough, which is consistent with past assessments of aerosol simulations over southern Africa [*Kinne et al.*, 2006]. The tropics are the main source of the positive SSA bias, which is important since the tropics are typically the part of southern Africa with the highest AOD (e.g., Figures 1–2). The extratropics have a slightly positive SSA bias, on average, but the spread in the comparison is large, making it difficult to draw any conclusions.

[25] The results in Figure 4 suggest that either the scattering component of the simulated aerosol (i.e., OM and sulfate in this region) [see *Ginoux et al.*, 2006] is too large or that the absorbing component (OM and black carbon, BC) is too small. The other possibility is that the optical properties of OM, sulfate, and BC, especially with regards to the imaginary component of the refractive index are biased [e.g., *Magi et al.*, 2007]. Uncertainties in UW SSA [*Magi et al.*, 2008] are significant (horizontal error bars in Figure 4), and may explain part of the discrepancy, but we explore a longer time series of SSA compared to AM2e in section 3.2 and show that the high bias in AM2e SSA is consistent over a much different temporal scale. Except for about four cases, neighboring grid cell variability of AM2e SSA (vertical error bars in Figure 4) is too small to explain the discrepancy.

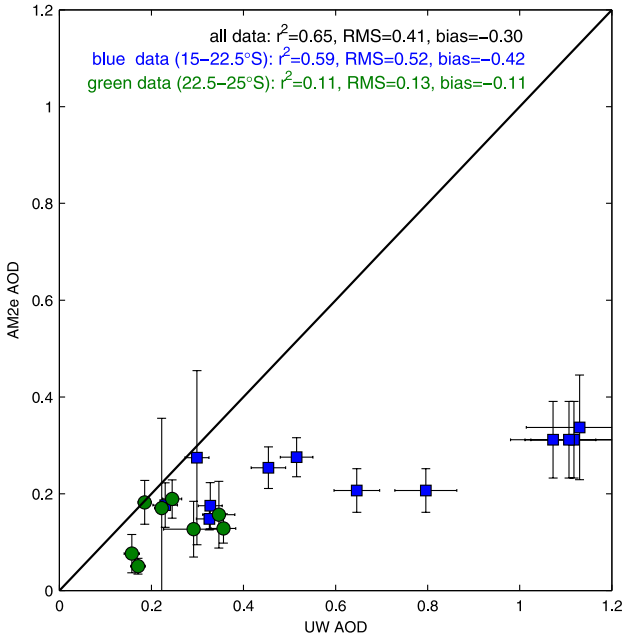

Figure 3. Comparison of AOD at a wavelength of 550 nm derived from measurements obtained from the University of Washington aircraft (UW AOD) with AOD output from AM2e (AM2e AOD). AM2e AOD at tropical latitudes are shown as blue squares (N = 12), and values at extratropical latitudes are green circles (N = 8). The vertical error bars are neighboring grid cell variability, the horizontal error bars are the total uncertainty in UW AOD, and the solid line is the one-to-one line.

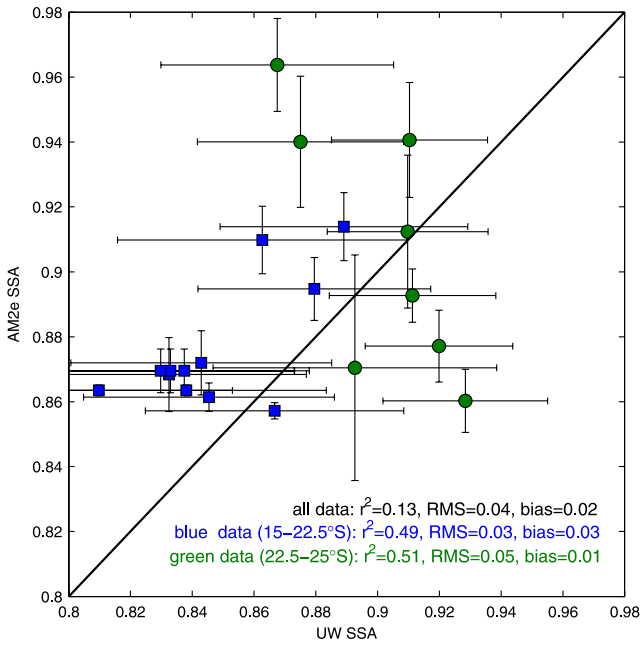

Figure 4. As per Figure 3, but for single scattering albedo (SSA) at a wavelength of 550 nm.

[26] The comparisons reveal that column AOD and SSA simulated by AM2e do not agree with measurements derived from the UW research aircraft. In Figure S1 of the auxiliary material, we show that vertical profiles of UW AOD and AM2e AOD do agree in terms of injection heights, where RMS differences are smaller at lower pressures.[1] This implies that simulated injection heights (based on *Dentener et al.* [2006]) are not an issue over southern Africa. Significant correlation coefficients in tropical southern Africa, where most of the burning occurs, suggest that relative AOD and SSA fluctuations appear to be captured by AM2e simulations. AOD fluctuations in the extratropics, however, are not significantly correlated, and SSA fluctuations are negatively correlated, which suggests that the timing of aerosol emissions in the simulation may be incorrect. In both the tropics and extratropics, the RMS difference between AM2e AOD and UW AOD is greater than 50%. AM2e SSA is biased high by 0.03 in the tropics and by 0.01 in the extratropics compared to UW SSA, noting that 11 out of 12 comparisons in the tropics are biased high.

[27] The discrepancies could simply be attributed to the difference in scale (both time and space) between an AM2e grid cell and a UW vertical profile. Most likely, UW aircraft data preferentially sampled areas with high aerosol loading since signal to noise requirements in the instruments was an issue, and some discrepancy is indeed expected since AOD fluctuations on small spatial scales can result in significant differences [*Anderson et al.*, 2003]. Fluctuations in regional SSA have never been characterized by in situ measurements. The comparisons do highlight a discrepancy in AM2e simulation of the tropical southern African aerosol, and raise questions about the driving forces of aerosol

[1] Auxiliary materials are available in the HTML. doi:10.1029/2008JD011128.

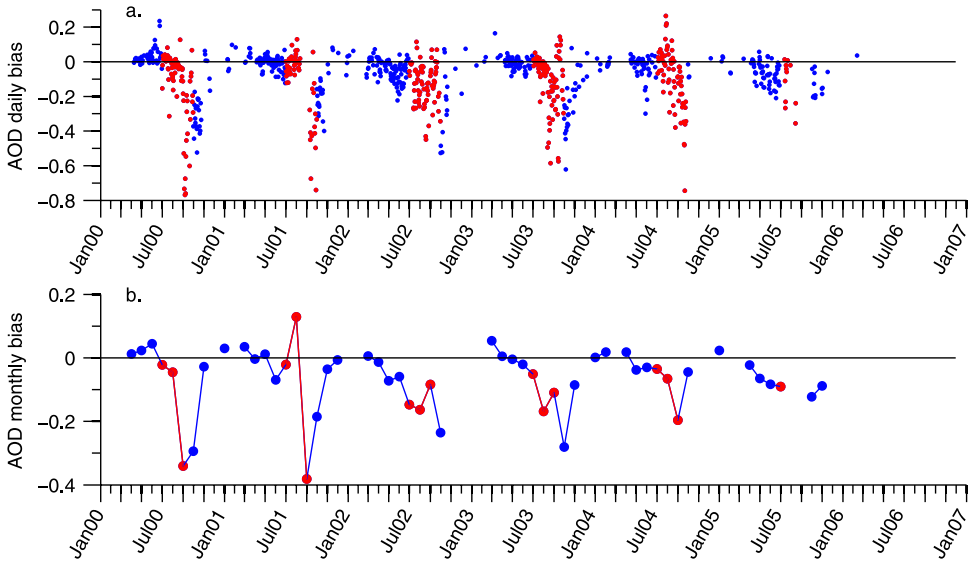

Figure 5. Comparison of (a) daily averaged and (b) monthly averaged AOD at a wavelength of 550 nm derived from AERONET measurements in Mongu, Zambia (latitude 15.25°S, longitude 23.15°E, elevation 1107 m) and output from AM2e for available data between January 2000 and December 2006. The AOD bias is calculated as AM2e−AERONET. Red circles and lines are during the biomass burning season (July, August, and September). Blue circles and lines are during the remainder of the year. Note the scale differences in the plots.

fluctuations in the extratropics (i.e., the insignificant correlation). Comparisons of UW AOD and UW SSA with AM2i AOD and AM2i SSA (not shown) are essentially the same as those shown in Figures 3–4. We explore longer AOD and SSA time series and broader spatial scale AOD data sets in the next sections to provide context for the comparisons with aircraft data and to examine whether the discrepancies are consistent.

3.2. AERONET

[28] We compiled AM2 daily and monthly output from 2000 to 2006 to compare with daily and monthly retrieved aerosol products (AOD and SSA) from ground-based NASA AERONET stations [*Holben et al.*, 2001; *Dubovik et al.*, 2002] in Mongu, Zambia (latitude 15.25°S, longitude 23.15°E, elevation 1107 m) and in Skukuza, South Africa (latitude 24.99°S, longitude 31.59°E, elevation 150 m). The Mongu station is at a tropical latitude in southern Zambia, and Skukuza is at an extratropical latitude in northeast South Africa (see Figure 1). Mongu and Skukuza have the longest time series of measurements in the region, making them the best choices to compare with model output. We use AERONET Level 2.0, Version 2.0 data products, which are processed using current algorithms and are quality controlled to exclude cloudy days and other events interfering with the retrieval (available at http://aeronet.gsfc.nasa.gov for more information). The AERONET stations are separated by about 1100 km, and the Mongu station is typically more strongly affected by local and regional biomass burning than Skukuza [*Eck et al.*, 2003].

[29] Similar to the aircraft measurements in section 3.1, the comparisons of AERONET products with AM2 output are limited since the spatial scales are so different. Using a longer time series of measurements from AERONET daily and monthly AOD, however, should average out some of the most local effects (like enhanced AOD from a fire near the AERONET station) and provide a better comparison. To construct the comparison, we use the two AM2 grid cells that encompass the two AERONET stations, but we also examine the neighboring grid cell variability of AM2 AOD around the central AERONET grid cell to examine whether the comparison significantly changes. Hypothetically, we would expect the agreement to be best in the monthly AOD comparison since AM2 uses a monthly inventory of biomass burning emissions. In all cases, there are significant gaps in the AERONET AOD time series due to failures in the retrieval algorithm for reasons discussed by *Dubovik et al.* [2002]. Most of the AERONET data corresponds to months affected by biomass burning since the atmosphere is more stable and dry (i.e., there are fewer cases of cloud contamination). We also restrict the monthly AOD comparison to AERONET monthly averages derived from three or more available days, which again slightly reduces the sample space.

3.2.1. Aerosol Optical Depth

[30] We present the time series of the difference between AM2e AOD and AERONET AOD at the tropical station (henceforth, Mongu AOD) in Figure 5. The RMS difference between daily averaged AM2e AOD and Mongu AOD in Figure 5a is 0.17 for all available comparison points, and is 0.12 in the monthly comparison in Figure 5b. As discussed in section 1, we found that the months with peak fire activity are July to September and we will refer to this as the "biomass burning season." If we restrict the comparison to biomass burning season (red circles in Figure 5), the RMS difference in daily AOD is 0.22 and is 0.16 in the monthly AOD comparison. The RMS difference is consistent throughout the year in terms of percent of the mean AOD and improves from about 85–100% different in the daily comparison to 65–75% different in the monthly comparison.

Table 2. Statistics From the Comparison of AM2 With AERONET Aerosol Optical Depth and Single Scattering Albedo, Both at a Wavelength of 550 nm[a]

AERONET Station, AM2 Configuration[b]	All Data Points						
	r^2	RMS[c]	Bias[d]	Minimum Bias	Maximum Bias	Mean AM2[e]	Mean AERONET[f]
Aerosol Optical Depth							
Daily							
Mongu, AM2e	0.43	0.17	−0.09	−1.22	0.26	0.14	0.23
Mongu, AM2i	0.43	0.17	−0.08	−1.22	0.27	0.14	0.23
Skukuza, AM2e	0.34	0.12	−0.05	−0.69	0.24	0.13	0.17
Skukuza, AM2i	0.34	0.12	−0.05	−0.68	0.27	0.13	0.17
Monthly[g]							
Mongu, AM2e	0.63	0.12	−0.07	−0.38	0.13	0.13	0.19
Mongu, AM2i	0.64	0.12	−0.06	−0.38	0.13	0.13	0.19
Skukuza, AM2e	0.45	0.06	−0.02	−0.21	0.09	0.13	0.15
Skukuza, AM2i	0.46	0.06	−0.02	−0.20	0.08	0.14	0.15
Single Scattering Albedo							
Daily							
Mongu, AM2e	0.10	0.06	0.03	−0.12	0.24	0.89	0.86
Mongu, AM2i	0.09	0.07	0.03	−0.12	0.23	0.89	0.86
Skukuza, AM2e	0.03	0.07	0.03	−0.16	0.24	0.91	0.89
Skukuza, AM2i	0.03	0.07	0.02	−0.16	0.25	0.91	0.89
Monthly[g]							
Mongu, AM2e	0.26	0.06	0.03	−0.09	0.13	0.90	0.87
Mongu, AM2i	0.26	0.06	0.03	−0.09	0.13	0.90	0.87
Skukuza, AM2e	0.09	0.07	0.05	−0.07	0.13	0.93	0.88
Skukuza, AM2i	0.09	0.07	0.05	−0.07	0.13	0.93	0.88
AERONET Station, AM2 Configuration[b]	Biomass Burning Data Points[h]						
	r^2	RMS[c]	Bias[d]	Minimum Bias	Maximum Bias	Mean AM2[e]	Mean AERONET[f]
Aerosol Optical Depth							
Daily							
Mongu, AM2e	0.32	0.22	−0.12	−1.22	0.26	0.20	0.32
Mongu, AM2i	0.32	0.22	−0.12	−1.22	0.27	0.20	0.32
Skukuza, AM2e	0.35	0.16	−0.06	−0.69	0.20	0.16	0.23
Skukuza, AM2i	0.35	0.16	−0.06	−0.68	0.20	0.16	0.23
Monthly[g]							
Mongu, AM2e	0.42	0.16	−0.11	−0.38	0.13	0.19	0.30
Mongu, AM2i	0.43	0.16	−0.11	−0.38	0.13	0.19	0.30
Skukuza, AM2e	0.41	0.09	−0.05	−0.21	0.04	0.16	0.21
Skukuza, AM2i	0.45	0.08	−0.05	−0.20	0.04	0.16	0.21
Single Scattering Albedo							
Daily							
Mongu, AM2e	0.01	0.07	0.06	−0.06	0.18	0.88	0.83
Mongu, AM2i	0.01	0.07	0.06	−0.06	0.18	0.88	0.83
Skukuza, AM2e	0.12	0.06	0.04	−0.09	0.24	0.90	0.87
Skukuza, AM2i	0.12	0.06	0.03	−0.09	0.25	0.90	0.87
Monthly[g]							
Mongu, AM2e	*0.01*	*0.07*	*0.06*	*0.01*	*0.13*	*0.88*	*0.82*
Mongu, AM2i	*0.01*	*0.07*	*0.06*	*0.01*	*0.13*	*0.88*	*0.82*
Skukuza, AM2e	*0.09*	*0.07*	*0.06*	*0.01*	*0.13*	*0.91*	*0.85*
Skukuza, AM2i	*0.08*	*0.07*	*0.06*	*0.01*	*0.13*	*0.91*	*0.85*

[a]We compare AM2 output from two grid cells that are colocated with two AERONET stations in southern hemisphere Africa (Mongu and Skukuza). Italicized values indicate correlation that is not statistically significant ($p > 0.05$). The information in this table are derived from data in Figures 5–8.
[b]Mongu, Zambia is located at 15.25°S, 23.15°E, 1107 m; Skukuza, South Africa is at 24.99°S, 31.59°E, 150 m.
[c]RMS is root-mean-squared difference.
[d]Bias is defined as AM2 AOD – AERONET AOD.
[e]Mean AM2 refers to mean AOD and SSA from either AM2e (externally mixed aerosol) or AM2i (internally mixed black carbon and sulfate).
[f]AERONET AOD uncertainty is estimated as 0.01, and SSA uncertainty is 0.03 for AOD $\geq$ 0.2 [*Dubovik et al.*, 2002].
[g]Monthly AERONET AOD comparisons are only for monthly AOD with three or more data points.
[h]Biomass burning season is defined here as July to September.

[31] Both AM2e AOD and Mongu AOD show an increase in AOD during the biomass burning season by about 50% above the annual mean AOD, but on average, AM2e AOD is biased low by 0.07 to 0.12. The mean bias masks large fluctuations in the monthly bias during the entire time series, ranging from −0.38 to 0.13 during the entire year, with the largest biases occurring during the biomass burning season (Table 2). Neighboring AM2e grid cell variability in AOD accounts for about ±10% change in the RMS difference, but this does not explain the discrepancies of 65–100% in AM2e AOD compared with AERONET AOD. Similarly, neighboring grid cell variability only accounts for about ±10% of the 40–50% negative bias in AM2e AOD.

[32] The time series of the bias between AM2e AOD and the AERONET AOD at the extratropical station (henceforth, Skukuza AOD) in Figure 6 reveals smaller-scale fluctuations in the monthly bias, ranging from −0.21 to 0.04 during the biomass burning season (Table 2). On average, the monthly

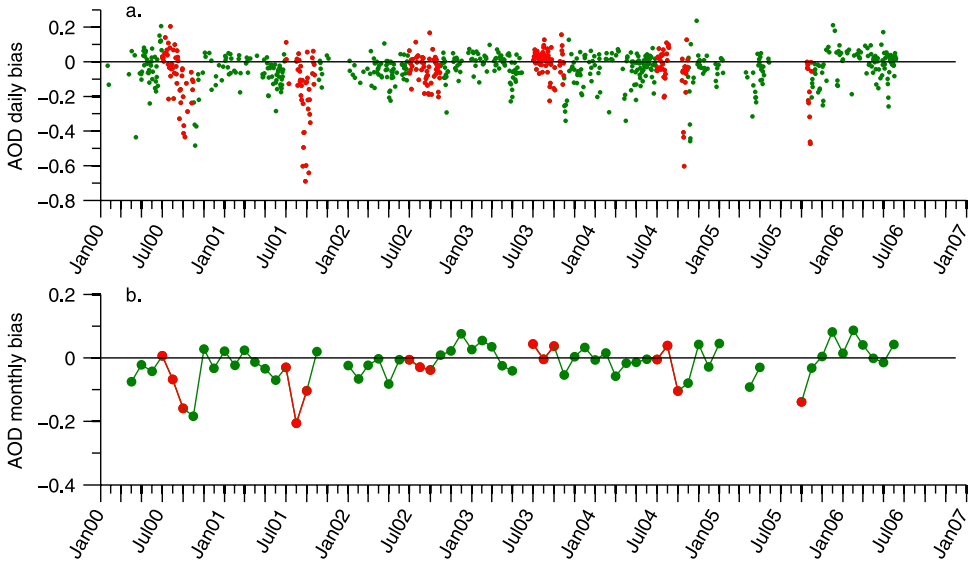

Figure 6. As per Figure 5, but showing the comparison of (a) daily averaged and (b) monthly averaged AOD at a wavelength of 550 nm from AERONET measurements in Skukuza, South Africa (latitude 24.99°S, longitude 31.59°E, elevation 150 m) with AM2e AOD. The AOD bias is calculated as AM2e−AERONET. Red circles and lines are during the biomass burning season (July, August, and September). Green circles and lines are during the remainder of the year. Note the scale differences in the plots.

AM2e AOD is biased low by 0.05 during the biomass burning season, while the daily bias is −0.06 (but with a larger range of −0.69 to +0.20). The RMS difference in the monthly AOD is 0.09 during the biomass burning season, which is about half of the RMS difference between AM2e AOD and Mongu AOD of 0.16. Neighboring AM2e grid cell variability in AOD accounts for less than ±10% change in both the RMS difference, but this again does not explain the discrepancies of 40−80% in AM2e AOD compared with AERONET AOD. Neighboring grid cell variability accounts for about ±20% of the 10−30% negative bias in AM2e AOD, so may be a significant part of the discrepancy during most of the year.

[33] This negative bias in AM2e AOD in both the tropics and the extratropics compared to AERONET (Figures 5−6) is consistent with the comparison with UW aircraft data shown in Figure 3. However, the magnitudes of both the RMS difference and the bias in the AERONET comparison are smaller. This is most likely due to the better spatial representation of AERONET retrieval products relative to aircraft, when compared to a model grid cell. Also, like the comparisons in section 3.1, the statistics of AM2i AOD compared to AERONET AOD (both Mongu and Skukuza) are virtually identical to the statistics of AM2e AOD compared to AERONET AOD (Table 2). This again indicates that even for a longer time series of AOD, the internal mixing of BC and sulfate in AM2i does not improve the discrepancy.

3.2.2. Single Scattering Albedo

[34] In Figure 7, we show the time series of the bias of AM2e SSA compared to Mongu SSA for both daily and monthly averages. AM2e SSA is biased high by, on average, 0.02 to 0.06 for all comparisons (Table 2), with a larger bias during the biomass burning season (red circles in Figure 7). RMS difference is larger than the bias (ranging from 0.06 to 0.07), which is due to the large fluctuations in the bias throughout the year in the positive and negative directions. The range of the bias improves from −0.12 to 0.24 in the daily comparison to −0.09 to 0.13 in the monthly comparison (i.e., high and low biases are averaged out), but otherwise the monthly comparison is nearly the same as the daily comparison. During the biomass burning season in particular, it is rare that that AM2e is biased low in SSA. The correlation in the time series ranges from 0.01 to 0.26, with no significant correlation during the biomass burning season.

[35] Finally, we show the time series of the bias of AM2e SSA compared to Skukuza SSA in Figure 8. AM2e SSA is biased high by 0.03 to 0.05 throughout the entire year and by 0.04 to 0.06 during the biomass burning season (Table 2). RMS differences are greater than the biases (ranging from 0.06 to 0.07), because there is high variability in the bias throughout the year. The range of the bias improves from −0.16 to 0.24 in the daily comparison to −0.07 to 0.12 in the monthly comparison, but the mean bias in the monthly comparison is a factor of two larger than the mean bias in the daily comparison. The correlation in the time series ranges from 0.03 to 0.12, with no significant correlation during the monthly biomass burning season data. It is rare that that AM2e is biased low in SSA, but during the biomass burning season (red points in Figure 8), there are no cases when monthly SSA is biased low.

[36] The high bias in AM2e SSA is consistent with the comparison of UW SSA with AM2e SSA in Figure 4. This again suggests that the simulated aerosol is not absorbing enough in the extratropics or the tropics where the burning primarily occurs. Another similarity in the comparisons in Figures 4, 7, and 8 is the very poor correlation. The simulated AOD is much better correlated with AERONET AOD (which is the opposite of the comparison with UW AOD) than the simulated SSA, indicating perhaps that the emissions are timed reasonably well, but that the chemical

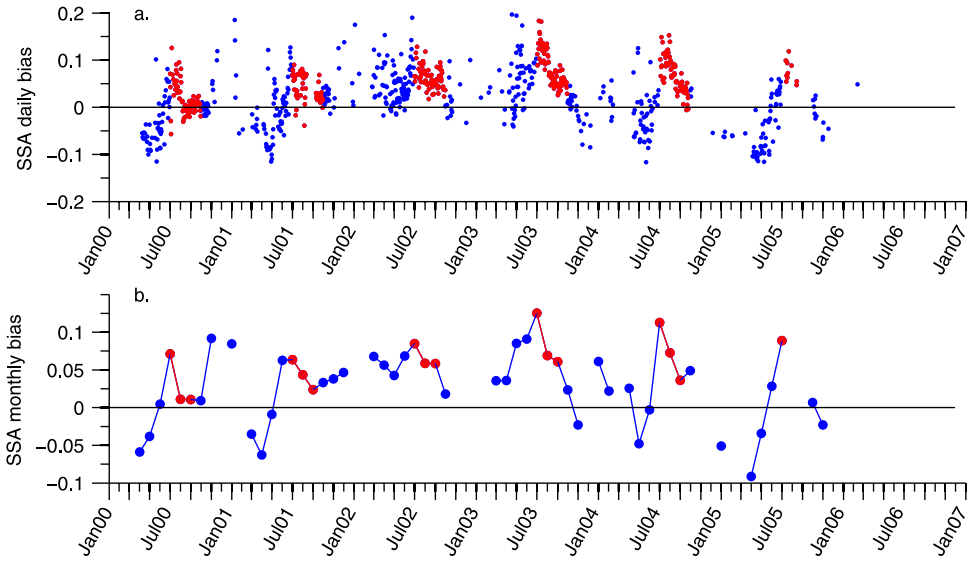

Figure 7. As per Figure 5, but for SSA. The SSA bias is calculated as AM2e−AERONET.

composition or aerosol optical properties used to convert from mass are incorrect.

[37] Finally, just like the comparison with UW SSA, AM2i SSA derived using internally mixed BC and sulfate has little or no impact on the comparisons with Mongu and Skukuza SSA. We do not show the comparison with AM2i, but list the statistics of both AM2 configurations compared with both AERONET stations in Table 2. An aerosol mixing scheme that includes the significant OM component, or perhaps a different mixing assumption [e.g., *Chylek et al.*, 1988], may be necessary to make significant improvements in AM2 simulations over southern Africa, but these refinements are beyond the scope of this study.

3.3. MODIS

[38] Finally, we compare daily, monthly, and seasonally averaged AOD over southern Africa from MODIS satellite retrievals of AOD (henceforth, MODIS AOD) with AM2 AOD. For seasonally averaged AOD, we use January–March, April–June, July–September, and October–December, such that the biomass burning season (July–September) is captured together, noting the caveats we discussed in section 1 about this choice. MODIS products are available since March 2000, so we examine about 7 years of data from March 2000 to December 2006 (similar to the time series we examined for the AERONET and AM2 comparison) using only the collection 5 version of the MODIS daily AOD aggregated to 1° by 1° grid boxes [*Levy et al.*, 2007]. We then average all land-based AOD from MODIS and from AM2 over southern hemisphere tropical Africa (0° to 20°S, referred to as the "tropics") and southern hemisphere extratropical Africa ("extratropics," 20° to 40°S). These comparisons provide a much larger spatial comparison to help assess the simulation of regional AOD.

[39] The statistics from all the comparisons (both AM2e and AM2i versus MODIS) are listed in Table 3. AM2 AOD

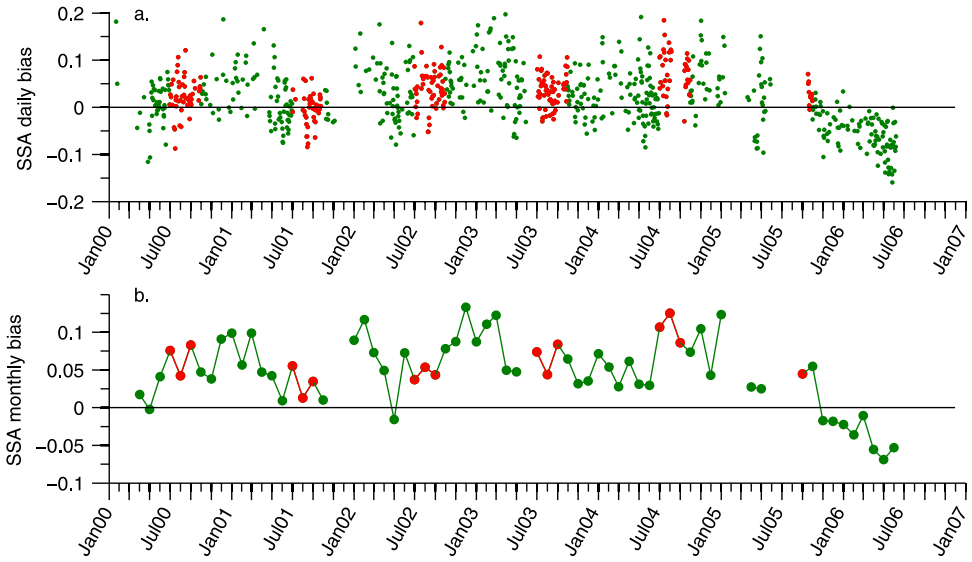

Figure 8. As per Figure 6, but for SSA. The SSA bias is calculated as AM2e−AERONET.

Table 3. Statistics From the Comparison of Aerosol Optical Depth at a Wavelength of 550 nm From AM2 and MODIS Averaged Over Tropical and Extratropical Latitudes of Southern Hemisphere Africa Land Surfaces[a]

Region, AM2 Configuration[b]	r^2	RMS[c]	Bias[d]	Minimum Bias	Maximum Bias	Mean AM2[e]	Mean MODIS[f]
				All Data Points			
Daily							
Tropics, AM2e	0.44	0.11	−0.08	−0.44	0.10	0.14	0.22 ± 0.08
Tropics, AM2i	0.43	0.11	−0.08	−0.43	0.11	0.15	0.22 ± 0.08
Extratropics, AM2e	0.44	0.04	−0.01	−0.34	0.12	0.11	0.12 ± 0.07
Extratropics, AM2i	0.45	0.04	−0.01	−0.33	0.13	0.11	0.12 ± 0.07
Monthly							
Tropics, AM2e	0.54	0.11	−0.09	−0.26	0.03	0.14	0.23 ± 0.08
Tropics, AM2i	0.53	0.10	−0.08	−0.25	0.03	0.15	0.23 ± 0.08
Extratropics, AM2e	0.56	0.03	−0.02	−0.14	0.05	0.11	0.13 ± 0.07
Extratropics, AM2i	0.57	0.03	−0.01	−0.14	0.05	0.12	0.13 ± 0.07
Seasonal[g]							
Tropics, AM2e	0.62	0.09	−0.08	−0.15	−0.01	0.15	0.23 ± 0.08
Tropics, AM2i	0.62	0.09	−0.08	−0.15	0.00	0.15	0.23 ± 0.08
Extratropics, AM2e	0.45	0.03	−0.02	−0.09	0.02	0.11	0.13 ± 0.07
Extratropics, AM2i	0.47	0.03	−0.02	−0.08	0.03	0.12	0.13 ± 0.07
				Biomass Burning Data Points[h]			
Daily							
Tropics, AM2e	0.23	0.14	−0.10	−0.44	0.10	0.19	0.29 ± 0.09
Tropics, AM2i	0.21	0.13	−0.10	−0.43	0.11	0.19	0.29 ± 0.09
Extratropics, AM2e	0.45	0.04	−0.001	−0.25	0.12	0.12	0.12 ± 0.07
Extratropics, AM2i	0.46	0.04	0.003	−0.25	0.13	0.12	0.12 ± 0.07
Monthly							
Tropics, AM2e	0.38	0.12	−0.10	−0.26	−0.001	0.19	0.30 ± 0.09
Tropics, AM2i	0.35	0.12	−0.10	−0.25	0.005	0.20	0.30 ± 0.09
Extratropics, AM2e	0.63	0.03	0.002	−0.04	0.05	0.13	0.13 ± 0.07
Extratropics, AM2i	0.63	0.03	0.007	−0.03	0.05	0.14	0.13 ± 0.07
Seasonal[g]							
Tropics, AM2e	*0.21*	*0.09*	*−0.08*	*−0.11*	*−0.05*	*0.20*	*0.28 ± 0.09*
Tropics, AM2i	*0.16*	*0.08*	*−0.08*	*−0.10*	*−0.04*	*0.21*	*0.28 ± 0.09*
Extratropics, AM2e	*0.23*	*0.02*	*−0.003*	*−0.03*	*0.02*	*0.13*	*0.13 ± 0.07*
Extratropics, AM2i	*0.21*	*0.02*	*0.002*	*−0.02*	*0.03*	*0.14*	*0.13 ± 0.07*

[a]Values that are italicized indicate a correlation that is not statistically significant ($p > 0.05$). The information in this table are derived from data in Figures 9–10.
[b]"Tropics" refer to southern hemisphere tropical Africa; "extratropics" refer to southern hemisphere extratropical Africa.
[c]RMS is root-mean-squared difference.
[d]Bias is defined as AM2 AOD − MODIS AOD.
[e]Mean AM2 refers to mean AOD and SSA from either AM2e (externally mixed aerosol) or AM2i (internally mixed black carbon and sulfate).
[f]MODIS AOD uncertainty is calculated as 0.05 ± 0.15 × AOD per *Remer et al.* [2005].
[g]Seasons are January–March, April–June, July–September, October–December; hence, the biomass burning season is July–September and there are only seven comparison points.
[h]Biomass burning season is defined here as July to September.

is biased low in nearly every case. The time series comparisons are all significantly correlated over the course of the entire year ($r^2 = 0.43$ to 0.62, $p < 0.05$). The mean values of AM2 AOD and MODIS AOD agree to within the published uncertainty in MODIS AOD of 0.05 ± 0.15 × AOD [*Remer et al.*, 2005] in the extratropics. The tropics again show a much larger discrepancy, where the range of AOD bounded by MODIS uncertainty rarely encompasses the mean AM2e AOD, especially during the biomass burning season. The range of the bias improves by about 50% from the daily to monthly comparison in the tropical comparison, which is consistent with the fact that AM2e uses a monthly biomass burning inventory as input. Mean RMS differences (compared to the mean) are on the order of 40–60% in the tropics and 10–40% in the extratropics.

[40] We show the time series comparison of AM2e AOD and MODIS AOD in the tropics and the extratropics in Figures 9 and 10, respectively. The emissions during the biomass burning season results in a significant peak in both AM2e AOD and MODIS AOD. The peak in AM2e AOD, however, occurs roughly one month prior to the peak in MODIS AOD, which is most clear in the monthly comparison. This is consistent in both the tropics and the extratropics, although it more evident in the tropics. The time series of AM2i AOD is so close to that of AM2e AOD (see the statistics in Table 3), that we did not include it on Figures 9–10. We explore possible reasons for the phase difference in AM2 AOD compared to MODIS AOD in section 4.

4. Analysis

[41] The tropics are where the majority of fires occur (Figure 1), and where AOD is highest both at a local and regional scale (Figures 2, 3, 5, 9), but the tropics are also where the discrepancies of AM2e AOD compared with available data are largest in the southern Africa region. There is a clear trend showing that the RMS differences and biases improve as we change scales from the very limited temporal and spatial scale of aircraft data to a better temporal

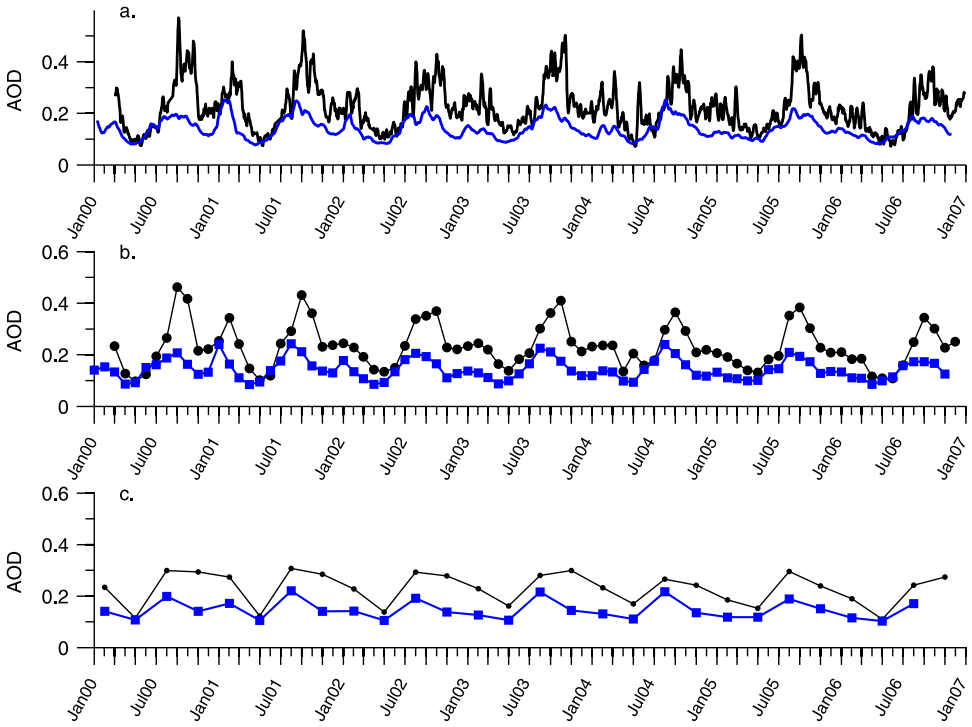

Figure 9. Comparison of (a) daily averaged, (b) monthly averaged, and (c) seasonally averaged AOD at a wavelength of 550 nm retrieved from MODIS satellite measurements (black) and derived from AM2e output (blue) from January 2000 to December 2006. The AOD is averaged over land surfaces in Southern Hemisphere tropical Africa.

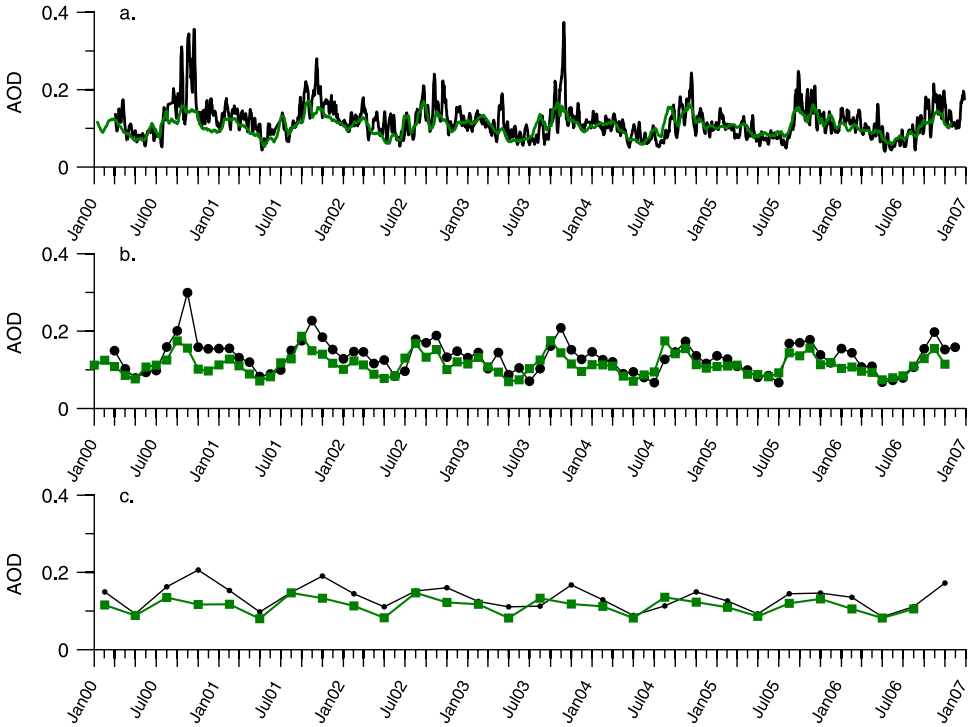

Figure 10. As per Figure 9, but AOD is averaged over land surfaces in Southern Hemisphere extratropical Africa and AM2e output is shown in green. Also, note that the scale is different than Figure 9.

Table 4. Summary of Comparisons of Monthly Aerosol Optical Depth From AERONET, MODIS, and Single Scattering Albedo From AERONET, With AM2 Optical Properties, All at Wavelengths of 550 nm[a]

	Tropical	Extratropical
	Aerosol Optical Depth	
AERONET	0.30 ± 0.16	0.21 ± 0.09
AM2e	0.19 ± 0.06	0.16 ± 0.03
AM2i	0.19 ± 0.07	0.16 ± 0.03
MODIS	0.30 ± 0.08	0.13 ± 0.04
AM2e	0.19 ± 0.03	0.13 ± 0.03
AM2i	0.20 ± 0.03	0.14 ± 0.03
	Single Scattering Albedo	
AERONET	0.82 ± 0.03	0.85 ± 0.03
AM2e	0.88 ± 0.01	0.91 ± 0.02
AM2i	0.88 ± 0.01	0.91 ± 0.02

[a]For AERONET comparisons (aerosol optical depth (AOD) and single scattering albedo (SSA)), AM2e and AM2i refer to the grid cell-to-grid cell comparison (comparable to a single AERONET station), while they refer to regionally averaged AOD in the MODIS comparisons (directly comparable to MODIS). All data in this table applies to the biomass burning season (July to September), and the values are listed as the mean ± standard deviation.

resolution in the AERONET data to a regionally averaged comparison using the MODIS aerosol product (i.e., compare Figure 3 to Tables 2 and 3). All the data provide useful information, and the aircraft data could be especially useful in developing subgrid-scale parameterizations of aerosol characteristics. In general, although there is a clear biomass burning season in the simulated AOD, there are consistent discrepancies between model and data in the timing of the peak AOD and in the magnitudes of AOD and SSA in all the comparisons.

[42] The time series of AM2e AOD and MODIS AOD in Southern Hemisphere tropical Africa (Figure 9) shows that AM2e AOD increases twice during the course of each year; the first increase in AM2e AOD occurs in January, while the second increase begins in June and corresponds to the onset of the biomass burning season. This dual peak in AM2e AOD is consistent with MODIS AOD, with AM2e including a large peak in January 2001 that is similar to MODIS AOD. According to AM2e simulations, the January peaks in AOD are a result of dust intrusions from Northern Hemisphere Africa. AM2e AOD peaks about one month earlier than MODIS AOD which marks a timing discrepancy in the onset of the biomass burning season. GFED emissions [*van der Werf et al.*, 2006] used by AM2 to simulate biomass burning are tied to MODIS fire counts [*Giglio et al.*, 2003, 2006], so MODIS fire counts peak about one month earlier than MODIS AOD as well. MODIS AOD timing is consistent with AERONET AOD in the tropics (Figure 2a), suggesting that MODIS AOD is a realistic characterization of regional AOD. This indicates that either not enough aerosol is emitted in the model to match the peak AOD timing of MODIS or that the simulated aerosol sink is too strong.

[43] In addition to the timing discrepancy, we investigate the possible reasons for the discrepancies in the magnitudes of AOD and SSA. The evidence summarized in Table 4 shows that AM2 AOD in the tropics is underestimated by ~30–40% (compared to both AERONET and MODIS) and AM2e SSA in tropics is overestimated by ~8%. AOD in the extratropics is underestimated by over 20% compared to AERONET, but agrees well (within 1–6%) with the regionally averaged comparison with MODIS. The increase in the high AOD bias in the MODIS comparisons from 1 to 6% with AM2e and AM2i, respectively, is consistent with a simulated industrial source in eastern South Africa; AOD and absorption are likely enhanced by internally mixed biomass burning BC and industrial sulfate components. The better agreement of AM2 with the regional average (Table 4) than with the AERONET AOD (Table 4) most likely implies burning that impacts northeastern South Africa (see Figure 1) is not properly captured in AM2. Skukuza reports notably higher AOD during the biomass burning season than regionally averaged MODIS data, as we showed in Figure 2. Similar to the tropics, AM2 SSA in the extratropics is overestimated by 7% compared to AERONET. The SSA bias remains high since the AERONET grid box is not strongly impacted by industrial emissions to the south (i.e., there is still no strong source of sulfates).

[44] Internal mixing of sulfate and BC in AM2i (compared to AM2e) should be a more realistic representation of an aerosol in the ambient atmosphere and is consistent with in situ observations over southern Africa [*Li et al.*, 2003; *Posfai et al.*, 2003], but Table 4 suggests that SSA comparisons with AERONET are basically the same in AM2i and AM2e, with only a slight enhancement of AOD for the extratropical regional average (Table 4, AM2e versus AM2i). *Matichuk et al.* [2007] found better agreement with their simulations and AERONET SSA (from AERONET sites in Inhaca, Mozambique, and Ndola, Zambia) using internally mixed BC and OM, but their results only apply to September 2000. We expect that internally mixing OM with sulfate and BC aerosol would improve the comparisons in Africa (and other regions impacted by burning), but this is not currently a feature of the model. As it is, AM2i does not simulate SSA in southern Africa more accurately than AM2e in either the tropics or the extratropics.

4.1. Aerosol Mass

[45] One possible reason for discrepancies in AOD and SSA may be differences in aerosol mass compared with observations. In Figure 11, we show the AM2 mass concentrations for particulate matter less than 2.5 μm diameter (PM2.5), OM, sulfate, and BC in the lowest model layers (between the surface and about 500 hPa). AM2e and AM2i have identical mass distributions. On the basis of data collected during the SAFARI-2000 field campaign [*Eatough et al.*, 2003; *Formenti et al.*, 2003; *Gao et al.*, 2003; *Kirchstetter et al.*, 2003], OM and BC account for about 60–75% of the submicron aerosol mass in southern African regional haze during the biomass burning season. If semivolatile components of OC (SVOC) are included, the carbonaceous aerosol contribution to submicron aerosol mass could be as much as 85% [*Eatough et al.*, 2003]. Ammonium sulfate and ammonium nitrate contributions to submicron aerosol mass range from 10 to 40% [*Eatough et al.*, 2003; *Formenti et al.*, 2003].

[46] The PM2.5 mass from AM2 in Figure 11a is roughly comparable to the submicron aerosol mass referred to above because coarse mode (diameters > 1 μm) particles were not significant. The median contribution of OM and BC to PM2.5 aerosol mass during the biomass burning season is 55%, while the median sulfate contribution to aerosol mass during the biomass burning season is 26% (Figure S2 of the

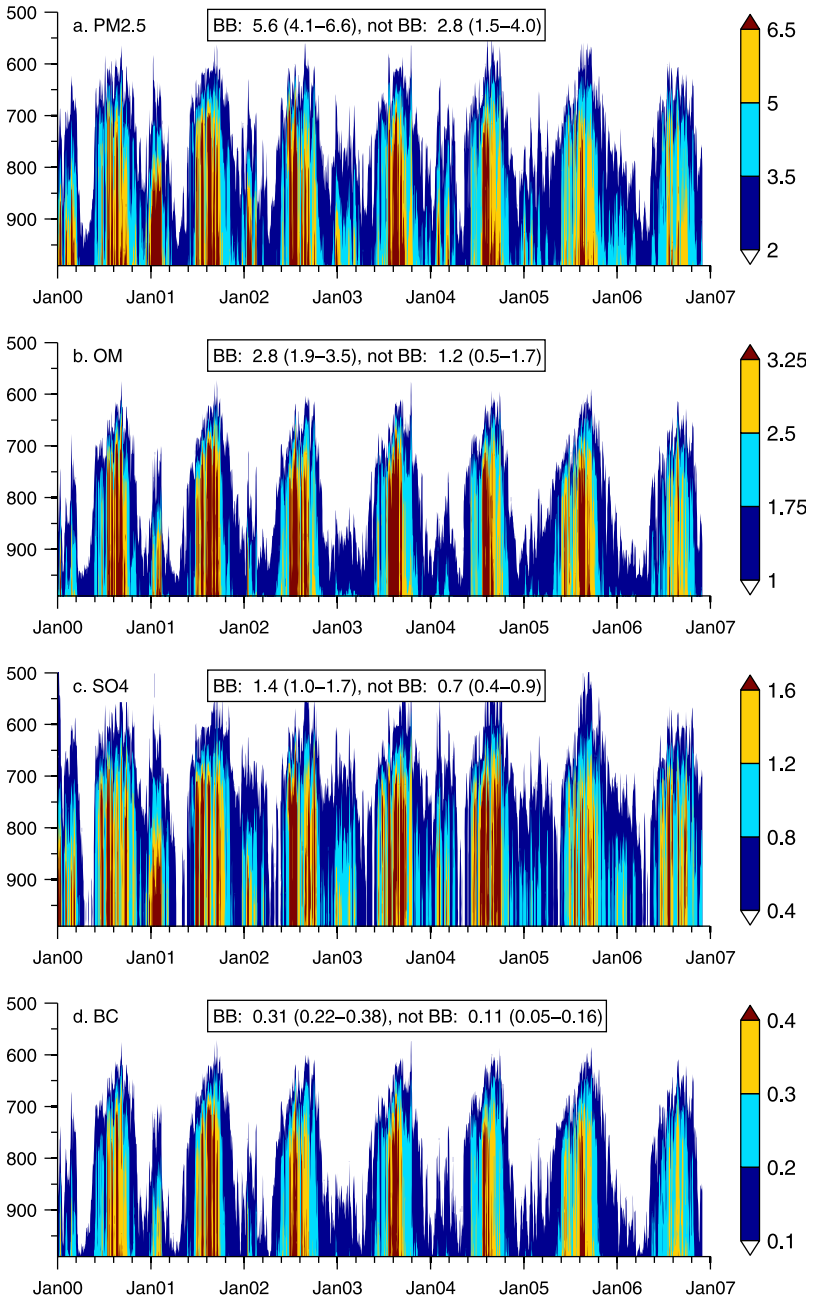

Figure 11. Time series of vertical profiles of aerosol mass concentrations (μg/m^3, in the color bars) of (a) particulate matter less than 2.5 μm diameter (PM2.5), (b) organic matter (OM), (c) sulfate (SO_4), and (d) black carbon (BC) simulated by AM2 (both AM2e and AM2i) and averaged over tropical southern Africa. The *y* axes show AM2 pressure levels (hPa). Mass statistics are listed in each plot as median and interquartile range of the individual chemical components during the biomass burning (BB) season (July–September) and during the rest of the year (not BB, all months but July–September). Note the scale differences in each plot.

auxiliary material). Dust accounts for the remainder of the simulated PM2.5 aerosol mass. Mass apportionment, therefore, suggests that OM and BC percent contributions are underestimated in AM2.

[47] On the other hand, absolute mass concentrations in AM2 are generally much different from what is reported by in situ studies in southern Africa, especially in the tropics. During the biomass burning season, PM2.5 aerosol mass in AM2 ranges from 1 to 12 μg/m^3 (median of 6 μg/m^3) while *Eatough et al.* [2003] and *Formenti et al.* [2003] suggest submicron aerosol mass ranges from about 15 to 75 μg/m^3 in regional hazes located far from direct sources of biomass burning emissions. OM and sulfate consistently account for the majority of AM2 AOD in both the tropics and extratropics (Figures S3–S4 of the auxiliary material), and both are well correlated with monthly MODIS AOD. The correlation is consistent with in situ evidence [*Formenti et al.*, 2003; *Gao et al.*, 2003] that biomass burning is a source of

OM and sulfate particles, but evidence also suggests that the contribution of carbonaceous matter to AOD is much higher than that of sulfate [*Eatough et al.*, 2003; *Kirchstetter et al.*, 2003]. OM mass ranges as high as 7.5 $\mu g/m^3$ in AM2 (median of 2.8 $\mu g/m^3$), while BC mass is as high as 0.8 $\mu g/m^3$ (median of 0.3 $\mu g/m^3$). Values of OM and BC reported by *Eatough et al.* [2003] range from about 10 to 56 $\mu g/m^3$ and 1 to 2 $\mu g/m^3$, respectively. The species mass concentrations in AM2 are considerably less than in situ measurements in the region suggest and may be part of the reason AM2 AOD does not agree with AOD from other sources. We investigate this in more detail below.

4.2. Aerosol Size and Relative Humidity

[48] The size distributions assumed in AM2 (Table 1 and section 2.2) affect AOD and SSA, so we examine the sensitivity of both to changes in aerosol size using offline calculations. We examine the impact of changes to the assumed geometric mean diameter (D_g) for sulfate, OM, and BC size distributions since these chemical species are the dominant controls on AOD and SSA fluctuations in southern Africa. We set up the sensitivity tests by varying D_g from 0.75 $\times$ D_g to 5 $\times$ D_g (and holding σ_g and total mass constant) where D_g corresponds to the values listed for sulfate, OM, and BC in Table 1. Using Mie theory, we calculate the mass extinction efficiencies and single scattering albedos (at 550 nm and RH = 50%), and then calculate AOD and SSA assuming a uniform distribution of aerosol between 0 and 6 km in the atmosphere. We assume a constant total mass concentration of 6 $\mu g/m^3$ with mass apportioned as 34% sulfate, 60% OM, and 6% BC, which is similar to median PM2.5 mass concentration and overall mass apportionment during the biomass burning season for AM2 as shown in Figure 11a.

[49] The case of 2 $\times$ D_g increases AOD by 15–21%. For 3 $\times$ D_g and beyond, the mass extinction efficiency begins to fall off for all the species, while for 1.25 $\times$ D_g, AOD increases by 11–12%. Considered alone, these increases in D_g suggest that the low AOD bias would improve. However, the impact on SSA is an increase of $\sim$5% from 0.75 $\times$ D_g to 2 $\times$ D_g for BC mass fractions near 6%. The percent increase is larger for contributions of BC greater than 6%. Thus, although increases in size can improve the low AOD bias, SSA biases become worse.

[50] These sensitivity tests are purely hypothetical arguments, and regardless of the results, should be considered in the context of the physical plausibility of increases in size. Namely, we have to ask the question: What range of values of D_g for sulfate, OM, and BC is consistent with observations? There are no studies that report chemically speciated size distributions in southern Africa. In terms of total aerosol size distributions reported for southern Africa, *Reid et al.* [2005a] list values of D_g ranging from 0.12 to 0.25 μm, *Magi et al.* [2007] suggest a range from 0.15 to 0.22 μm, and *Haywood et al.* [2003a] suggest $D_g = 0.24 \pm 0.02$ μm, which together imply that there is a broad range of "representative" size distributions. The total size distribution for AM2 (combining sulfate, OM, and BC in proportions stated above) can be described with $D_g \approx 0.11$ μm. Increasing D_g by a factor of two for OM and BC results in $D_g \approx 0.18$ μm. Both values fall within the range suggested by past research.

[51] Another aspect of aerosol size that may impact the simulated AOD and SSA is relative humidity (RH). In AM2, all sulfate grows as the RH increases, while only the hydrophilic part of the OM and BC components (section 2.2) grow in size. *Magi and Hobbs* [2003] showed that the southern African biomass burning aerosol is fairly hygroscopic, but that since RH is less than 50% throughout the lowest part of the troposphere, the effect of RH on aerosol optical properties is minimal [*Magi et al.*, 2008]. This is consistent with climate studies from southern hemisphere Africa showing that the biomass burning season is coincident with a dry atmosphere [*Garstang et al.*, 1996]. RH simulated by AM2 is correspondingly low in the tropics (Figure S5 of the auxiliary material) and throughout southern Africa during the biomass burning season. The effect of RH on AOD and SSA only becomes significant for RH > 50–60% [*Magi and Hobbs*, 2003], but the RH between about 500 hPa and the surface in AM2 averages around 40% during the biomass burning season, which is consistent with independent observations.

[52] To summarize, although RH growth does not explain the low bias in AOD over southern Africa, assumed size distributions of the chemical components simulated in AM2 can help explain the low bias in AOD. On the basis of offline calculations, we suggest that doubling OM and BC geometric mean diameters (D_g) increases AOD by about 15–21%, accounting for more than half the low bias, depending on the region. The new values of D_g are still within the range of D_g suggested by the literature. More than doubling D_g results in a decrease in the extinction efficiencies and the impact is smaller. However, SSA increases by about 4–5% when we double D_g, so the high SSA bias would become worse (higher). The same conclusions apply to increases in BC or OM D_g alone. The only way to drive SSA down (improving the high SSA bias) is to increase the contribution of BC to the total aerosol. We, however, have not tested these findings in AM2 where transport and deposition also play roles in controlling aerosol loading. Thus, the 15–21% increase in AOD should be considered an upper limit to the impact of size, and we conclude that size alone cannot explain the discrepancies.

4.3. Transport and Deposition

[53] Transport into and out of the tropics may also be an important factor in determining AM2 AOD. Convective transport is weak during the dry season owing to the presence of persistent stable layers and upper level subsidence [*Cosijn and Tyson*, 1996]. Advective transport plays a more important role [*Swap and Tyson*, 1999; *Garstang et al.*, 1996]. We test the role of transport by creating pulse experiments with AM2, where we simulate pulses of aerosol emissions from 15 July to 15 August (while setting other aerosol emissions to zero) from a subset of the southern African extratropics, southern African tropics, and northern African tropics. We then examine the simulated transport paths and residence times of the aerosol in the originating region and the impact on neighboring regions for about 45 days after the pulse ends (Figures S6–S7 of the auxiliary material), noting that nearly all the aerosol disappears after about 75 days.

[54] From these pulse experiments, we find that only a small fraction (4–5%) of OM aerosol (Figure S6 of the auxiliary material) emitted in the southern extratropics or the northern tropics is transported to the southern tropics.

There is more cross-boundary transport from the tropics, with about 57% of the aerosol staying over the region, 30% transported over the Atlantic Ocean, 10% to the extratropics, and 3% to the northern tropics. Transport toward the Atlantic Ocean agrees with climatologies of southern African transport pathways (e.g., the "Angolan plume" discussed by *Garstang et al.* [1996]) and is consistent with satellite data products [e.g., *Chin et al.*, 2002; *Kinne et al.*, 2006]. The small fraction of aerosol transported from the southern tropics to the extratropics seems to occur in episodes, probably related to brief synoptic disturbances.

[55] We also tested to see whether the impact of transport and deposition was similar for OM and sulfate (Figure S6 of the auxiliary material). Both species have similar transport pathways and times, but if OM is transported more quickly out of the source region, then this would result in OM (and BC) mass contributions to PM2.5 mass that are biased low. We found that slightly (but not significantly) more sulfate aerosol is transported from the tropics to the Atlantic (32%), extratropics (13%), and northern tropics (6%). Thus, only about 49% of the sulfate from the tropics stays over the tropics, compared to 57% of OM. If anything, the model favors more OM over the tropics. However, transport of sulfate aerosol from the extratropics to the tropics is about double that of transport of OM (12% compared to 5%), roughly balancing out the loss from the tropics.

[56] Finally, wet deposition has very little impact during the biomass burning season of southern Africa (see discussion of RH above). We tested this by running a pulse experiment with wet deposition on and off, and found that average aerosol mass was reduced by only ~6% by wet deposition over southern Africa. Thus, we conclude that simulated transport and deposition in the tropics and extratropics is consistent with observations and cannot explain the discrepancies between MODIS AOD and AM2 AOD. The low bias in AM2 AOD begins and ends in the tropics and the major aerosol source in this region is biomass burning.

4.4. Biomass Burning Emissions

[57] Finally, we examine the sensitivity of the comparisons to the biomass burning emissions from the GFED inventory [*van der Werf et al.*, 2006] used in AM2. Our intention here is to provide emissions that would improve the discrepancies with AERONET and MODIS. There is a great deal of uncertainty about biomass burning emissions due to a number of individually uncertain parameters needed to calculate the emissions. *Bond et al.* [2004] assessed emissions for a typical year in the 1990s, and their estimates of global BC + OM emissions are 19–90 Tg/a, while the range for GFED (1997–2006) is 28–52 Tg/a. If we apply uncertainties *Bond et al.* [2004] used to establish their range, then GFED emissions are 18–84 Tg/a. Thus, the natural variability predicted over a decade of GFED emissions, which include a strong ENSO event in 1997–1998, is much less than the confidence interval suggested by *Bond et al.* [2004]. One other estimate of emissions (for 2001) based on GFED with different emission factors by *Chin et al.* [2007] suggested emissions of 76 Tg/a, which is at the high end of the confidence interval suggested by *Bond et al.* [2004]. The range of BC/OM between the three studies is 8.6% to 12.4%, with *Bond et al.* [2004] slightly higher than the others.

[58] The magnitudes of simulated aerosol mass concentrations are dependent on emissions, but we also showed that the model underestimates the contribution of carbonaceous aerosol in southern Africa in sections 4.1 and 4.2. This suggests that emissions from GFED may be both too low and incorrectly partitioned. In other words, our comparisons with both AOD and SSA strongly suggest that GFED over southern Africa should not be universally scaled. More aerosol would certainly improve the low AOD bias, it is unlikely to improve the high SSA bias.

[59] In order to closely match the long AERONET time series in Mongu and Skukuza, we have to increase southern African biomass burning emissions of OM by 1.6 and BC by 3.8, which increases annual emissions from 10 Tg/a to 14 Tg/a. Globally, this is about 54 Tg/a, which is within the range predicted by *Bond et al.* [2004]. In a GCM study, *Sato et al.* [2003] tried to match model output to global AERONET climatologies and found that they had to increase OM by 1.6–1.8 and BC by 2.2–3.8, which is consistent with our findings in southern Africa. In a SAFARI-2000 study with an aerosol transport model, *Matichuk et al.* [2007] found that a 30% increase in GFED emissions improved comparisons of simulated AOD with available observations (like MODIS) for September 2000, while we found that a 47% increase was needed, noting, however, that our study period was much different. After increasing emissions, the high bias in SSA is almost zero for the Mongu comparisons, while Skukuza SSA is still biased high in AM2. AOD comparisons with MODIS and AERONET data also improve, which is not surprising. The correlations between the data products and AM2 output do not change significantly, implying there are still unresolved issues related to timing the emissions. Since we showed in Figure 2 that MODIS and AERONET AOD are significantly correlated, this suggests the timing is related to the emissions.

[60] The ratio of BC/OM over southern Africa is 18% in the emissions used to match simulated AOD and SSA, which is significantly higher than anything suggested by the published inventories. Referring to studies of in situ measurements, *Bond et al.* [2004] suggested a huge range of BC/OM of 6% to 89% with polluted areas in Asia around 25%. In situ data from Africa [*Kirchstetter et al.*, 2003] suggests BC/OM of about 16% (ranging from 3% to 48%), so the increase in BC/OM needed to match AERONET is consistent with measurements, but not with inventories.

[61] Part of the problem may be that models and inventories do not account for light-absorbing OM [*Kirchstetter et al.*, 2004; *Bond and Bergstrom*, 2006] in the simplified OM and BC approach, which is good example of two communities whose understandings of carbonaceous aerosols have yet to converge in a unified and consistent approach. We can only suggest, on the basis of our evidence that BC in models should be larger to account for important discrepancies in SSA. To account for discrepancies in both AOD and SSA, BC and OM should be increased, but disproportionately. There is literature support for all of this, but fundamental questions remain about how to simulate an absorbing aerosol.

4.5. Comparisons and Impacts

[62] Results presented in this study generally support the findings by *Ginoux et al.* [2006], which evaluated global

aerosol properties of a previous version of AM2. Both evaluations consistently reveal strong negative biases in AM2 AOD in southern Africa, especially during the biomass burning season. The configurations of AM2 in this study include several updates since the version of AM2 described by *Ginoux et al.* [2006] (see section 2), including an option to internally mix the BC and sulfate aerosol components in AM2i. The model in this study simulates the 2000–2006 aerosol to directly compare with measurements that are a temporal match and also includes an evaluation of SSA. *Ginoux et al.* [2006] evaluated AM2 simulations from 1996 to 2000 compared to climatologies of available data rather than direct temporal comparisons. Aside from methodological differences, however, the basic conclusions (low AOD bias and low bias in OM contribution to AOD) by *Ginoux et al.* [2006] about biomass burning regions still apply to the newer configurations of AM2 discussed here.

[63] The clear-sky radiative impact of the low bias in AOD and the high bias in SSA in AM2 compared to available observations implies that the magnitude of the top of the atmosphere radiative forcing (RF_{toa}) is slightly overestimated (too negative) and surface radiative forcing (RF_{sfc}) is underestimated (not negative enough) by AM2 over southern Africa. In a study of southern African aerosol radiative impacts, *Magi et al.* [2008] showed that a percentage change in SSA has 3–6 times the impact on RF_{toa} and RF_{sfc} than an equivalent percentage change in AOD. Thus, the high bias in SSA in AM2 will outweigh the low bias in AOD in terms of the impact on RF_{toa}, causing the magnitude of RF_{toa} to be greater than it would be from observations. We estimate, on the basis of results by *Magi et al.* [2008], that the total effect on RF_{toa} would be an ~8% increase in the magnitude (+21% from higher SSA and −13% from lower AOD) over the entire year, noting the individual impacts of the biases in SSA and AOD offset each other.

[64] The same biases act together to decrease the impact of the aerosol on the annual surface radiative flux over southern Africa, implying that AM2 has about 20% more solar radiation reaching the surface than observations suggest, and that the impact of the biases on the magnitude of RF_{sfc} during the burning season is not significantly larger (21%). The magnitude of RF_{sfc} by the AM2 aerosol is therefore less than that derived from observation. Slightly more than half of the impact is due to the lower AOD, while slightly less than half is due to higher SSA. The radiative energy absorbed in the atmosphere (i.e., $RF_{toa} - RF_{sfc}$) would be less in AM2 than suggested by observations as well. A full analysis of regional RF impacts due to apparent biases in AM2 is beyond the scope of this study, but may reveal larger-scale issues regarding the impacts of biases in aerosol optical properties.

5. Conclusions

[65] We evaluated the aerosol simulation from the second version of the Atmospheric Model (AM2) of the GFDL General Circulation Model in Southern Hemisphere Africa (southern Africa) against multiple data sources, comparing aerosol optical depth (AOD) and single scattering albedo (SSA) at a midvisible wavelength of 550 nm. We examined output from two configurations of AM2; AM2e has an externally mixed aerosol, while AM2i has internally mixed black carbon and sulfate aerosol components (section 2). The comparisons offered strong evidence that the simulation of biomass burning in tropical southern Africa in AM2 is inconsistent with in situ data collected from a research aircraft, retrieved AOD and SSA products (Level 2.0, Version 2.0) from NASA AERONET, and the retrieved AOD gridded product (collection 5) from the NASA MODIS satellite. Comparisons in extratropical southern Africa were generally much better in terms of AOD, but a time series comparison of SSA at an extratropical AERONET station revealed that AM2 SSA is biased significantly high.

[66] The simulation of biomass burning in tropical southern Africa is particularly important since MODIS fire counts from 2000 to 2006 reveal that the tropics account for over 90% of the fires that occur in all of southern Africa, and previous studies showed that southern African biomass burning accounts for a large part of the global carbonaceous aerosol emissions. Using comparisons at three spatial and temporal scales over southern Africa, we found that AM2 AOD is biased low by 30–40% in the tropics and 0–20% in the extratropics. The bias in the tropics is consistent throughout the year, but the bias in the extratropics during the biomass burning season varies from negative in the AERONET comparison to slightly positive in the MODIS comparison. We also showed that AM2 AOD peaks one month earlier than MODIS AOD nearly every year we examined, but we could not find a single explanation for this problem (see sections 4.3 and 4.4). AM2 SSA is biased high by 4–8% throughout the year, noting that in the tropics, AM2 SSA bias increases from 4% to 8% during the biomass burning season. Weak correlation with SSA, especially during the biomass burning season, suggests that the chemical composition or aerosol optical properties used to convert from mass concentrations are incorrect. SSA comparisons did not improve when we used a configuration of AM2 with internally mixed black carbon and sulfate aerosols.

[67] We concluded, after analyses of many different mechanisms impacting AOD and SSA (section 4) that an underestimate in carbonaceous aerosol mass over southern Africa is the most likely reason for the discrepancies presented in section 3. On the basis of a sensitivity test with the biomass burning emissions used as input to AM2 (GFED) [*van der Werf et al.*, 2006], we showed that discrepancies in AOD and SSA over southern Africa are minimized if organic and black carbon emissions from GFED biomass burning are increased by factors of 1.6 and 3.8, respectively. We suggested that the disproportionate increase required for black carbon emissions may be due to inadequate ability of models to simulate light absorbing organic carbon. This requires further study and better integration of modeling methodology with available measurements. Regardless of the reasons, it is difficult to assess the quality of climate model output at the regional scale until simulations and available measurements, especially aerosol optical properties, are in better agreement. Africa is particularly sensitive to discrepancies in the simulation of the regional aerosol since most of the emissions are not exported quickly.

[68] Underestimating aerosol emissions may impact climate predictions by next generation climate models that include both internal mixing and aerosol-cloud interactions. We estimated that the impact of the biases in the model would

result in a ~8% increase in the magnitude of the top of the atmosphere radiative forcing (making it too negative) and ~20% decrease in the magnitude of the surface radiative forcing (making it not negative enough) over southern Africa throughout the year, but we did not determine what effect this would have on general circulation or climate. If a choice has to be made, is it more important to accurately match aerosol emissions from available inventories or match simulated aerosol optical properties to available data products? Both are observationally based and both require some assumptions, but at least in this study, it appears that the models lose something in the translation of aerosol emissions to aerosol optical properties.

[69] **Acknowledgments.** We thank Brent Holben and Stuart Piketh for their efforts in establishing and maintaining the Mongu and Skukuza AERONET sites in southern Africa. We also thank members of the NASA community for maintaining the LAADS data archive (http://ladsweb.nascom.nasa.gov). Comments by Dilip Ganguly, Arnico Pandis, and three anonymous reviewers helped improve this project.

References

Anderson, T. L., R. J. Charlson, D. M. Winker, J. A. Ogren, and K. Holmen (2003), Mesoscale variations of tropospheric aerosols, *J. Atmos. Sci.*, *60*, 119–136, doi:10.1175/1520-0469(2003)060<0119:MVOTA>2.0.CO;2.

Andreae, M. O., C. D. Jones, and P. M. Cox (2005), Strong present-day aerosol cooling implies a hot future, *Nature*, *435*, 1187–1190, doi:10.1038/nature03671.

Anyamba, A., C. O. Justice, C. J. Tucker, and R. Mahoney (2003), Seasonal to interannual variability of vegetation and fires at SAFARI 2000 sites inferred from advanced very high resolution radiometer times series data, *J. Geophys. Res.*, *108*(D13), 8507, doi:10.1029/2002JD002464.

Arakawa, A., and W. H. Schubert (1974), Interaction of a cumulus cloud ensemble with the large-scale environment, part I, *J. Atmos. Sci.*, *31*, 674–701, doi:10.1175/1520-0469(1974)031<0674:IOACCE>2.0.CO;2.

Balkanski, Y. J., D. J. Jacob, G. M. Gardner, W. C. Graustein, and K. K. Turekian (1993), Transport and residence times of tropospheric aerosols inferred from a global three-dimensional simulation of ^{210}Pb, *J. Geophys. Res.*, *98*, 20,573–20,586.

Balkanski, Y., M. Schulz, T. Claquin, and S. Guibert (2007), Reevaluation of mineral aerosol radiative forcings suggests a better agreement with satellite and AERONET data, *Atmos. Chem. Phys.*, *7*, 81–95.

Bohren, C. F., and D. R. Huffman (1983), *Absorption and Scattering of Light by Small Particles*, 530 pp., John Wiley, New York.

Bond, T. C., and R. W. Bergstrom (2006), Light absorption by carbonaceous particles: An investigative review, *Aerosol Sci. Technol.*, *40*, 27–67, doi:10.1080/02786820500421521.

Bond, T. C., D. G. Streets, K. F. Yarber, S. M. Nelson, J. Woo, and Z. Klimont (2004), A technology-based global inventory of black and organic carbon emissions from combustion, *J. Geophys. Res.*, *109*, D14203, doi:10.1029/2003JD003697.

Chin, M., P. Ginoux, S. Kinne, O. Torres, B. N. Holben, B. N. Duncan, R. V. Martin, J. A. Logan, A. Higurashi, and T. Nakajima (2002), Tropospheric aerosol optical thickness from the GOCART model and comparisons with satellite and Sun photometer measurements, *J. Atmos. Sci.*, *59*, 461–483, doi:10.1175/1520-0469(2002)059<0461:TAOTFT>2.0.CO;2.

Chin, M., T. Diehl, P. Ginoux, and W. Malm (2007), Intercontinental transport of pollution and dust aerosols: Implications for regional air quality, *Atmos. Chem. Phys.*, *7*, 5501–5517.

Chylek, P., V. Srivastava, R. G. Pinnick, and R. T. Wang (1988), Scattering of electromagnetic waves by composite spherical particles: Experiment and effective medium approximations, *Appl. Opt.*, *27*, 2396–2404, doi:10.1364/AO.27.002396.

Cosijn, C., and P. D. Tyson (1996), Stable discontinuities in the atmosphere over South Africa, *S. Afr. J. Sci.*, *92*, 381–386.

Delworth, T. L., et al. (2006), GFDL's CM2 global coupled climate models. Part I: Formulation and simulation characteristics, *J. Clim.*, *19*, 643–674, doi:10.1175/JCLI3629.1.

Dentener, F., et al. (2006), Emissions of primary aerosol and precursor gases in the years 2000 and 1750, prescribed data-sets for AeroCom, *Atmos. Chem. Phys.*, *6*, 4321–4344.

Dubovik, O., B. Holben, T. F. Eck, A. Smirnov, Y. J. Kaufman, M. D. King, D. Tanre, and I. Slutsker (2002), Variability of absorption and optical properties of key aerosol types observed in worldwide locations, *J. Atmos. Sci.*, *59*, 590–608, doi:10.1175/1520-0469(2002)059<0590:VOAAOP>2.0.CO;2.

Eatough, D. J., N. L. Eatough, Y. Pang, S. Sizemore, T. W. Kirchstetter, T. Novakov, and P. V. Hobbs (2003), Semivolatile particulate organic material in southern Africa during SAFARI 2000, *J. Geophys. Res.*, *108*(D13), 8479, doi:10.1029/2002JD002296.

Eck, T. F., et al. (2003), Variability of biomass burning aerosol optical characteristics in southern Africa during the SAFARI 2000 dry season campaign and a comparison of single scattering albedo estimates from radiometric measurements, *J. Geophys. Res.*, *108*(D13), 8477, doi:10.1029/2002JD002321.

Formenti, P., W. Elbert, W. Maenhaut, J. Haywood, S. Osborne, and M. O. Andreae (2003), Inorganic and carbonaceous aerosols during the Southern African Regional Science Initiative (SAFARI 2000) experiment: Chemical characteristics, physical properties, and emission data for smoke from African biomass burning, *J. Geophys. Res.*, *108*(D13), 8488, doi:10.1029/2002JD002408.

Gao, S., D. A. Hegg, P. V. Hobbs, T. W. Kirchstetter, B. I. Magi, and M. Sadilek (2003), Water-soluble organic components in aerosols associated with savanna fires in southern Africa: Identification, evolution, and distribution, *J. Geophys. Res.*, *108*(D13), 8491, doi:10.1029/2002JD002324.

Garstang, M., P. D. Tyson, R. Swap, M. Edwards, P. Kallberg, and J. A. Lindesay (1996), Horizontal and vertical transport of air over southern Africa, *J. Geophys. Res.*, *101*, 23,721–23,736, doi:10.1029/95JD00844.

GFDL Global Atmospheric Model Development Team (2004), The new GFDL global atmosphere and land model AM2–LM2: Evaluation with prescribed SST simulations, *J. Clim.*, *17*, 4641–4673, doi:10.1175/JCLI-3223.1.

Giglio, L., J. Descloitres, C. O. Justice, and Y. J. Kaufman (2003), An enhanced contextual fire detection algorithm for MODIS, *Remote Sens. Environ.*, *87*(2–3), 273–282, doi:10.1016/S0034-4257(03)00184-6.

Giglio, L., G. R. van der Werf, J. T. Randerson, G. J. Collatz, and P. Kasibhatla (2006), Global estimation of burned area using MODIS active fire observations, *Atmos. Chem. Phys.*, *6*, 957–974.

Ginoux, P., M. Chin, I. Tegen, J. M. Prospero, B. Holben, O. Dubovik, and S. Lin (2001), Sources and distributions of dust aerosols simulated with the GOCART model, *J. Geophys. Res.*, *106*, 20,255–20,273, doi:10.1029/2000JD000053.

Ginoux, P., L. W. Horowitz, V. Ramaswamy, I. V. Geogdzhayev, B. N. Holben, G. Stenchikov, and X. Tie (2006), Evaluation of aerosol distribution and optical depth in the Geophysical Fluid Dynamics Laboratory coupled model CM2.1 for present climate, *J. Geophys. Res.*, *111*, D22210, doi:10.1029/2005JD006707.

Giorgi, F., and W. L. Chameides (1986), Rainout lifetimes of highly soluble aerosols and gases as inferred from simulations with a general circulation model, *J. Geophys. Res.*, *91*, 14,367–14,376.

Guenther, A., R. Monson, and R. Fall (1991), Isoprene and monoterpene emission rate variability: Observations with eucalyptus and emission rate algorithm development, *J. Geophys. Res.*, *96*, 10,799–10,808, doi:10.1029/91JD00960.

Haywood, J. M., and V. Ramaswamy (1998), Global sensitivity studies of the direct radiative forcing due to anthropogenic sulfate and black carbon aerosols, *J. Geophys. Res.*, *103*, 6043–6058, doi:10.1029/97JD03426.

Haywood, J. M., S. R. Osborne, P. N. Francis, A. Keil, P. Formenti, M. O. Andreae, and P. H. Kaye (2003a), The mean physical and optical properties of regional haze dominated biomass burning aerosol measured from the C-130 aircraft during SAFARI 2000, *J. Geophys. Res.*, *108*(D13), 8473, doi:10.1029/2002JD002226.

Haywood, J., P. Francis, O. Dubovik, M. Glew, and B. Holben (2003b), Comparison of aerosol size distributions, radiative properties, and optical depths determined by aircraft observations and Sunphotometers during SAFARI 2000, *J. Geophys. Res.*, *108*(D13), 8471, doi:10.1029/2002JD002250.

Hess, M., P. Koepke, and I. Schult (1998), Optical properties of aerosols and clouds: The software package OPAC, *Bull. Am. Meteorol. Soc.*, *79*, 831–844, doi:10.1175/1520-0477(1998)079<0831:OPOAAC>2.0.CO;2.

Hobbs, P. V., P. Sinha, R. J. Yokelson, I. T. Bertschi, D. R. Blake, S. Gao, T. W. Kirchstetter, T. Novakov, and P. Pilewskie (2003), Evolution of gases and particles from a savanna fire in South Africa, *J. Geophys. Res.*, *108*(D13), 8485, doi:10.1029/2002JD002352.

Holben, B. N., et al. (2001), An emerging ground-based aerosol climatology: Aerosol optical depth from AERONET, *J. Geophys. Res.*, *106*, 12,067–12,097, doi:10.1029/2001JD900014.

Horowitz, L. W., et al. (2003), A global simulation of tropospheric ozone and related tracers: Description and evaluation of MOZART, version 2, *J. Geophys. Res.*, *108*(D24), 4784, doi:10.1029/2002JD002853.

Intergovernmental Panel on Climate Change (IPCC) (2007), *Climate Change 2007: The Physical Science Basis. Contribution of Working Group I to the Fourth Assessment Report of the Intergovernmental Panel*

on Climate Change, edited by S. Solomon et al., Cambridge Univ. Press, Cambridge, U. K.

Ito, A., A. Ito, and H. Akimoto (2007), Seasonal and interannual variations in CO and BC emissions from open biomass burning in Southern Africa during 1998 to 2005, *Global Biogeochem. Cycles*, *21*, GB2011, doi:10.1029/2006GB002848.

Johnson, B. T., S. R. Osborne, J. M. Haywood, and M. A. J. Harrison (2008), Aircraft measurements of biomass burning aerosol over West Africa during DABEX, *J. Geophys. Res.*, *113*, D00C06, doi:10.1029/2007JD009451.

Kinne, S., et al. (2006), An AeroCom initial assessment: Optical properties in aerosol component modules of global models, *Atmos. Chem. Phys.*, *6*, 1815–1834.

Kirchstetter, T. W., T. Novakov, P. V. Hobbs, and B. Magi (2003), Airborne measurements of carbonaceous aerosols in southern Africa during the dry, biomass burning season, *J. Geophys. Res.*, *108*(D13), 8476, doi:10.1029/2002JD002171.

Kirchstetter, T. W., T. Novakov, and P. V. Hobbs (2004), Evidence that the spectral dependence of light absorption by aerosols is affected by organic carbon, *J. Geophys. Res.*, *109*, D21208, doi:10.1029/2004JD004999.

Levy, R. C., L. A. Remer, S. Mattoo, E. F. Vermote, and O. Dubovik (2007), Second-generation operational algorithm: Retrieval of aerosol properties over land from inversion of Moderate Resolution Imaging Spectroradiometer spectral reflectance, *J. Geophys. Res.*, *112*, D13211, doi:10.1029/2006JD007811.

Li, F., P. Ginoux, and V. Ramaswamy (2008), Distribution, transport, and deposition of mineral dust in the Southern Ocean and Antarctica: Contribution of major sources, *J. Geophys. Res.*, *113*, D10207, doi:10.1029/2007JD009190.

Li, J., M. Posfai, P. V. Hobbs, and P. R. Buseck (2003), Individual aerosol particles from biomass burning in southern Africa: Part 2. Compositions and aging of inorganic particles, *J. Geophys. Res.*, *108*(D13), 8484, doi:10.1029/2002JD002310.

Lin, S.-J. (2004), A ''vertically Lagrangian'' finite-volume dynamical core for global models, *Mon. Weather Rev.*, *132*, 2293–2307, doi:10.1175/1520-0493(2004)132<2293:AVLFDC>2.0.CO;2.

Magi, B. I., and P. V. Hobbs (2003), Effects of humidity on aerosols in southern Africa during the biomass burning season, *J. Geophys. Res.*, *108*(D13), 8495, doi:10.1029/2002JD002144.

Magi, B. I., P. V. Hobbs, B. Schmid, and J. Redemann (2003), Vertical profiles of light scattering, light absorption and single-scattering albedo during the dry, biomass burning season in southern Africa and comparisons of in situ and remote sensing measurements of aerosol optical depth, *J. Geophys. Res.*, *108*(D13), 8504, doi:10.1029/2002JD002361.

Magi, B. I., Q. Fu, and J. Redemann (2007), A methodology to retrieve self-consistent aerosol optical properties using common aircraft measurements, *J. Geophys. Res.*, *112*, D24S12, doi:10.1029/2006JD008312.

Magi, B. I., Q. Fu, J. Redemann, and B. Schmid (2008), Using aircraft measurements to estimate the magnitude and uncertainty of the shortwave direct radiative forcing of southern African biomass burning aerosol, *J. Geophys. Res.*, *113*, D05213, doi:10.1029/2007JD009258.

Matichuk, R. I., P. R. Colarco, J. A. Smith, and O. B. Toon (2007), Modeling the transport and optical properties of smoke aerosols from African savanna fires during the Southern African Regional Science Initiative campaign (SAFARI 2000), *J. Geophys. Res.*, *112*, D08203, doi:10.1029/2006JD007528.

Ming, Y., and L. M. Russell (2004), Organic aerosol effects on fog droplet spectra, *J. Geophys. Res.*, *109*, D10206, doi:10.1029/2003JD004427.

Monahan, E. C., D. E. Spiel, and K. L. Davidson (1986), A model of marine aerosol generation via whitecaps and wave disruption, in *Oceanic Whitecaps and Their Role in Air-Sea Exchange Processes*, edited by E. C. Monahan and G. Mac Niocaill, pp. 167–174, D. Reidel, Dordrecht, Netherlands.

Moorthi, S., and M. J. Suarez (1992), Relaxed Arakawa-Schubert: A parameterization of moist convection for general circulation models, *Mon. Weather Rev.*, *120*, 978–1002, doi:10.1175/1520-0493(1992)120<0978:RASAPO>2.0.CO;2.

Posfai, M., R. Simonics, J. Li, P. V. Hobbs, and P. R. Buseck (2003), Individual aerosol particles from biomass burning in southern Africa: Part 1. Compositions and size distributions of carbonaceous particles, *J. Geophys. Res.*, *108*(D13), 8483, doi:10.1029/2002JD002291.

Prospero, J. M., P. Ginoux, O. Torres, and S. Nicholson (2002), Environmental characterization of global sources of atmospheric soil dust derived from the NIMBUS 7 Total Ozone Mapping Spectrometer (TOMS) absorbing aerosol product, *Rev. Geophys.*, *40*(1), 1002, doi:10.1029/2000RG000095.

Reddy, R. S., and O. Boucher (2004), A study of the global cycle of carbonaceous aerosols in the LMDZT general circulation model, *J. Geophys. Res.*, *109*, D14202, doi:10.1029/2003JD004048.

Reid, J. S., R. Koppmann, T. F. Eck, and D. P. Eleuterio (2005a), A review of biomass burning emissions part II: Intensive physical properties of biomass burning particles, *Atmos. Chem. Phys.*, *5*, 799–825.

Reid, J. S., T. F. Eck, S. A. Christopher, R. Koppmann, O. Dubovik, D. P. Eleuterio, B. N. Holben, E. A. Reid, and J. Zhang (2005b), A review of biomass burning emissions part III: Intensive optical properties of biomass burning particles, *Atmos. Chem. Phys.*, *5*, 827–849.

Remer, L. A., et al. (2005), The MODIS aerosol algorithm, products and validation, *J. Atmos. Sci.*, *62*, 947–973, doi:10.1175/JAS3385.1.

Ruellan, S., H. Cachier, A. Gaudichet, P. Masclet, and J. Lacaux (1999), Airborne aerosols over central Africa during the Experiment for Regional Sources and Sinks of Oxidants (EXPRESSO), *J. Geophys. Res.*, *104*, 30,673–30,690, doi:10.1029/1999JD900804.

Sato, M., J. Hansen, D. Koch, A. Lacis, R. Ruedy, O. Dubovik, B. Holben, M. Chin, and T. Novakov (2003), Global atmospheric black carbon inferred from AERONET, *Proc. Natl. Acad. Sci. U. S. A.*, *100*, 6319–6324, doi:10.1073/pnas.0731897100.

Schmid, B., et al. (2003), Coordinated airborne, spaceborne, and ground-based measurements of massive, thick aerosol layers during the dry season in southern Africa, *J. Geophys. Res.*, *108*(D13), 8496, doi:10.1029/2002JD002297.

Scholes, R. J., D. E. Ward, and C. O. Justice (1996), Emissions of trace gases and aerosols due to vegetation burning in southern hemisphere Africa, *J. Geophys. Res.*, *101*, 23,677–23,682, doi:10.1029/95JD02049.

Schwartz, S. E. (2004), Uncertainty requirements in radiative forcing of climate change, *J. Air Waste Manage. Assoc.*, *54*, 1351–1359.

Swap, R. J., and P. D. Tyson (1999), Stable discontinuities as determinants of the vertical distribution of aerosols and trace gases in the atmosphere, *S. Afr. J. Sci.*, *95*, 63–71.

Swap, R. J., H. J. Annegarn, J. T. Suttles, M. D. King, S. Platnick, J. L. Privette, and R. J. Scholes (2003), Africa burning: A thematic analysis of the Southern African Regional Science Initiative (SAFARI 2000), *J. Geophys. Res.*, *108*(D13), 8465, doi:10.1029/2003JD003747.

Tang, I. N., and H. R. Munkelwitz (1994), Water activities, densities, and refractive indices of aqueous sulfates and sodium nitrate droplets of atmospheric importance, *J. Geophys. Res.*, *99*, 18,801–18,808, doi:10.1029/94JD01345.

Tang, I. N., A. C. Tridico, and K. H. Fung (1997), Thermodynamic and optical properties of sea-salt aerosols, *J. Geophys. Res.*, *102*, 23,269–23,276, doi:10.1029/97JD01806.

Tie, X., S. Madronich, S. Walters, D. P. Edwards, P. Ginoux, N. Mahowald, R.-Y. Zhang, C. Lou, and G. Brasseur (2005), Assessment of the global impact of aerosols on tropospheric oxidants, *J. Geophys. Res.*, *110*, D03204, doi:10.1029/2004JD005359.

van der Werf, G. R., J. T. Randerson, G. J. Collatz, L. Giglio, P. S. Kasibhatla, A. F. Arellano Jr., S. C. Olsen, and E. S. Kasischke (2004), Continental-scale partitioning of fire emissions during the 1997 to 2001 El Nino/La Nina period, *Science*, *303*, 73–76, doi:10.1126/science.1090753.

van der Werf, G. R., J. T. Randerson, L. Giglio, G. J. Collatz, P. S. Kasibhatla, and A. F. Arellano Jr. (2006), Interannual variability in global biomass burning emissions from 1997 to 2004, *Atmos. Chem. Phys.*, *6*, 3423–3441.

Wesely, M. L. (1989), Parameterization of surface resistance to gaseous dry deposition in regional-scale numerical models, *Atmos. Environ.*, *23*, 1293–1304, doi:10.1016/0004-6981(89)90153-4.

P. Ginoux, Y. Ming, and V. Ramaswamy, Geophysical Fluid Dynamics Laboratory, NOAA, Princeton, NJ 08540, USA.

B. I. Magi, Atmospheric and Oceanic Sciences Program, Princeton University, Princeton, NJ 08544, USA. (brian.magi@noaa.gov)